الجمـــهورية الجزائرية الديمـــقراطية الشعـــبية

PEOPLE'S DEMOCRATIC REPUBLIC OF ALGERIA

وزارة التعـلـيـم الـعـالـــي والـبـحـث الـعـلـمي

MINISTRY OF HIGHER EDUCATION AND SCIENTIFIC RESEARCH

جـامـعـة عمّـــار ثـلـيـــجـــي بالاغـــــــــواط

AMAR THELIDGI- LAGHOUAT UNIVERSITY

كـلـيـــــة التكنولوجـــــــــا

FACULTY: OF TECHNOLOGY

قســـم الالكترونيك

DEPARTMENT: ELECTRONICS

MASTER'S THESIS

Directed by: BELHOUARI Sara

SAOUDI Aya

FIELD: Technology

SPECIALTY: Networks and Telecommunications

Theme

Low complexity of PTS Technique for PAPR Reduction of OFDM modulation in wireless communications fifth Generation

---

Last name and First Name:	Grade :	Quality:
Mr MERAH Hocine	MCA	Supervisor
Mr SGHIER Abedelkarim	MAA	Co- Supervisor
Mr MERAH Lahcene	Pr	President
Mr RAMDANI Al-Saadi	MAA	Examiner

Promotion: 2024/2025

Acknowledgements

This work is part of the graduation project that was set up at the level of the electronics department of the Amar Thaliji University Centre in Laghouat.

First of all, we thank Almighty God without His will nothing is possible, who has given us the help, the courage and the patience to do this work.

We would like to warmly thank our thesis supervisor Mr. MERAH HOCINE and Mr.SEGHIER ABED AL KARIM for her patience, her efforts and especially her wise advice which helped to fuel our reflection.

A big thank you to all our teachers from the Department of Electronics at Ammar Thaliji University and to all my friends.

Finally, we express our gratitude to all the people who have contributed directly or indirectly to the smooth running of this modest work.

Dedication

I dedicate this humble work:

To my dear mother

I see in you the perfect mother, always ready to sacrifice herself for the happiness of her children. Thank you for always supporting and encouraging me during these school years.

Thank you for everything mom.

To my late father.

Your love and your concern for me will mark me forever. I dedicate this graduation to your soul, may God have mercy on you.

And to my beautiful brothers and sisters. This work testifies to my attachment and my love. May God protect you.

To my family, my loved ones and those who give me love and life.

To all my friends who have always encouraged me and to whom I wish a lot of success; to all those I love.

Belhaouari Sara

Dedication

To those who planted the seeds of ambition in my heart and nurtured them with love and prayers until they blossomed into success...

To my dear parents, my guiding light in life, who never withheld anything from me, and were my unwavering support in every step.

To my mother… the source of tenderness, strength, and the greatest blessing life has given me.

To my father… from whom I learned that ambition knows no limits.

To my brothers and sisters, who were the warmth in cold days and the smile in times of fatigue.

To my esteemed professors, who generously shared their knowledge and guidance.

To my loyal friends, companions of the journey and success.

To everyone who crossed my path and left a beautiful trace in my life...

I dedicate to you the fruit of my effort and years of perseverance, hoping to always live up to your expectations.

Saoudi Aya

Résumé

Face à la demande croissante de débits élevés et de communications fiables dans les réseaux sans fil de cinquième génération (5G), l'importance des techniques de modulation efficaces s'est accrue. Ce mémoire se concentre sur une technique à faible complexité de séquence de transmission partielle (PTS) pour la réduction du rapport crête sur moyenne (PAPR) dans les systèmes OFDM. Un PAPR élevé entraîne une inefficacité énergétique et des distorsions non linéaires qui dégradent la performance du système. L'approche proposée permet une réduction significative du PAPR tout en minimisant la complexité computationnelle, ce qui la rend adaptée aux applications pratiques en 5G. Les résultats de simulation confirment l'efficacité de la méthode, promettant une meilleure efficacité énergétique et une intégrité du signal améliorée dans les communications sans fil futures.

Mots clés: OFDM, 5G, PAPR, HPA, PTS.

Abstract

The ever-increasing demand for high data rates and reliable communication in fifth-generation (5G) wireless networks has highlighted the importance of efficient modulation techniques. This thesis focuses on a low-complexity Partial Transmit Sequence (PTS) technique aimed at reducing the Peak-to-Average Power Ratio (PAPR) in Orthogonal Frequency Division Multiplexing (OFDM) systems. High PAPR in OFDM causes power inefficiency and nonlinear distortions, which degrade system performance. The proposed low-complexity approach achieves significant PAPR reduction while minimizing computational overhead, making it suitable for practical 5G implementations. Simulation results validate the effectiveness of the method, promising enhanced power efficiency and improved signal integrity in future wireless communications.

Keywords: OFDM, 5G, PAPR, HPA, PTS.

ملخص

مع تزايد الحاجة إلى معدلات بيانات عالية واتصالات موثوقة في شبكات الجيل الخامس(5G) ، أصبحت تقنيات التضمين الفعالة ضرورية للغاية. تركز هذه الرسالة على تقنية تسلسل الإرسال الجزئي (PTS) منخفضة التعقيد بهدف تقليل نسبة الذروة إلى المتوسط للطاقة (PAPR) في أنظمة التضمين بتقسيم التردد المتعامد .(OFDM) تسبب نسبة PAPR العالية في OFDM عدم كفاءة في استخدام الطاقة وتشويهات غير خطية تؤثر على أداء النظام. تُحقق الطريقة المقترحة تقليلًا ملحوظًا في PAPR مع تقليل العبء الحسابي، مما يجعلها مناسبة للتطبيقات العملية في أنظمة الجيل الخامس. تؤكد نتائج المحاكاة فعالية التقنية، مما يعد بتحسين كفاءة الطاقة وجودة الإشارة في الاتصالات اللاسلكية المستقبلية.

الكلمات المفتاحية: OFDM, 5G, PAPR, HPA, PTS.

Table of contents

Thanks I

Dedication II

Dedication III

Summary IV

Table of contents V

List of figures VIII

List of tables X

List of abbreviations XI

General introduction

Chapter 1: OFDM modulation and PAPR analysis

1.1 Introduction 04

1.2 Digital transmission Chain 04

1.3 Communication channels 05

1.3.1 Gaussian white noise channel 05

1.3.2 Multipath channel 06

1.3.3 Propagation Channel 06

1.4 Multi-Carrier Modulation 07

1.5 Principle of OFDM Modulation 07

1.5.1 OFDM system 07

1.5.2 Transmitter and Digital Modulator of an OFDM System 10

1.6 OFDM modulation has not only advantages but also disadvantages 13

1.7 Insertion of the cycle prefix 13

1.8 Peak to average power ratio (PAPR) of OFDM Signal 15

1.8.1 Definition of PAPR 15

1.8.2 Characterization of the PAPR of an OFDM Signal 16

1.9 Conclusion 17

Chapter 2: The High Power Amplifier (HPA)

2.1 Introduction 19

2.2 Power Amplifiers Overview 19

2.2.1 Definition 19

2.2.2 Characterization of the Power Amplifier: AM/AM and AM/PM Conversions 19

2.3 Key Parameters of the Power Amplifier 20
2.3.1 Power Efficiency 20
2.3.2 Input Back-Off and Output Back-Off 21
2.4 Operating Classes of the Power Amplifier 23
2.5 Behavioural Modeling of an Amplifier 24
2.5.1 Saleh Model 24
2.5.2 Rapp Model 24
2.6 Measurement of Distortions 25
2.6.1 Adjacent Channel Power Ratio (ACPR) 25
2.6.2 Error Vector Magnitude (EVM) 25
2.7 Effect of power amplifier on communications systems 26
2.7.1 Effect on the spectrum 27
2.7.2 Effect on the bit error rate 28
2.8 Conclusion 30

Chapter3: Low Complexity PTS for PAPR Reduction

3.1 Introduction 32
3.2 Conventional PTS Technique 32
3.2.1 Principle of PTS 32
3.2.2 PTS Sub-block Partitioning Methods 33
3.2.3 Search Complexity 33
3.3 Partial Transmission Sequence Method 34
3.3.1 PTS technique for PAPR reduction of OFDM signal 34
3.3.2 PTS technique for the reduction of the PAPR of the FBMC-OQAM signal 37
3.4 New PTS technique for the reduction of the PAPR of the OFDM signal 41
3.4.1 New-PTS 42
3.4.2 Complexity reduction technique 45
3.5 Analysis of the computational complexity for the New-PTS and C-PTS techniques 47
3.6 Conclusion 49

Chapter 4: Simulation results

4.1 Introduction 50
4.2 Objectives of the simulation 50
4.3 Simulation Results and Discussion 51

4.3.1 Performance of Methods for PAPR Reduction 51
4.3.2 BER Performance of the OFDM System 57
4.4 Conclusion 60
Conclusion General 62
Bibliographies 63

List of figures

Figure 1.1	Block diagram of a digital transmission chain	05
Figure 1.2	Representation of a channel in BBAG	05
Figure 1.3	Illustration of the phenomenon of multiple paths on the radio-mobile channel	06
Figure 1.4	Analog modulator of an OFDM symbol	08
Figure 1.5	Orthogonality between carriers or subcarriers of an OFDM system	09
Figure 1.6	Analog demodulator of an OFDM system	09
Figure 1.7	Digital Modulator/Demodulator of an OFDM system with Cyclic Prefix (CP)	11
Figure 1.8	Block diagram of CP-OFDM modulation	14
Figure 1.9	Spectra of the different carriers	14
Figure 2.1	Shape of the AM/AM Curve of a Power Amplifier	20
Figure 2.2	Simplified Power Balance of a Power Amplifier	21
Figure 2.3	Key Parameters of a Power Amplifier	22
Figure 2.4	Calculation of ACPR	25
Figure 2.5	Calculation of the EVM	26
Figure 2.6	Effect of the power amplifier on the constellation points	27
Figure 2.7	EVM as a function of input back off (IBO) for different SNR values	28
Figure 2.8	Effect of the power amplifier on the spectrum for different values of IBO	29
Figure 2.9	Effect of power amplifier on BER for different IBO value	29
Figure 3.1	Schematic diagram of the PTS	35
Figure 3.2	Example of partitioning a symbol into sub-blocks for the application of the technical PTS	36
Figure 3.3	Overlapping symbols in the FBMC-OQAM system	39
Figure 3.4	Functional diagram of the new PTS (New-PTS)	44
Figure 4.1	Comparison of PAPR reduction performance of the O-PTS, ABC-PTS, RS-PTS, BFO-PTS, GD-PTS, and I-PTS techniques, as well as the original OFDM signal, for 16-QAM	52
Figure 4.2	Comparison of PAPR reduction performance of the O-PTS, ABC-PTS, RS-PTS, BFO-PTS, GD-PTS, and I-PTS techniques, as well as the original OFDM signal, for QPSK……..	53
Figure 4.3	Comparison of PAPR reduction performance of the CR-New-PTS technique	54

for different values of the parameters W, V, and V_a for 16-QAM…….

Figure 4.4 Comparison of PAPR reduction performance of the CR-New-PTS technique for different values of the parameters W, V, and V_a for QPSK……. 55

Figure 4.5 Comparison of PAPR reduction performance of the O-PTS, CR-New-PTS, ABC-PTS, BFO-PTS, GD-PTS, and I-PTS techniques, as well as the original OFDM signal, for 16-QAM…….. 56

Figure 4.6 Comparison of PAPR reduction performance of the O-PTS, CR-New-PTS, ABC-PTS, BFO-PTS, GD-PTS, and I-PTS techniques, as well as the original OFDM signal, for QPSK……. 56

Figure 4.7 BER performance of the OFDM system using CR-New-PTS and O-PTS with QPSK modulation, when an HPA is applied over an AWGN channel……. 58

Figure 4.8 BER performance of the OFDM system using CR-New-PTS and O-PTS with 16-QAM modulation, when an HPA is applied over an AWGN channel…….. 59

Figure 4.9 BER performance of the OFDM system using CR-New-PTS and O-PTS with QPSK modulation, when an HPA is applied over a Rayleigh channel……. 59

Figure 4.10 BER performance of the OFDM system using CR-New-PTS and O-PTS with 16-QAM modulation, when an HPA is applied over a Rayleigh channel……. 60

List of tables

Table 2.1	Characterization of the Operating Classes of Power Amplifiers	24
Table 2.2	Example of ACPR measurement according to IBO values	29
Table 3.1	CCRR of the New-PTS compared to the C-PTS	48
Table 4.1	Simulation Parameters	51
Table 4.2	Complexity analysis of the different PTS techniques	57

List of acronyms and abbreviations

OFDM	Orthogonal Frequency Division Multiplexing
PAPR	Peak to Average Power Ratio
AWGN	Additive White Gaussian Noise
CDMA	Code Division Multiple Access
IFFT	Inverse Fast Fourier Transform
IDFT	Inverse Discrete Fourier Transform
CP	Cyclic Prefix
ISI	Inter-Symbol Interference
COFDM	Coded Orthogonal Frequency Division Multiplexing
DVB-T	Digital Video Broadcasting - Terrestrial
CCDF	Complementary Cumulative Distribution Function
HPA	High Power Amplifier
ACPR	Adjacent Channel Power Ratio
SNR	Signal to Noise Ratio
EVM	Error Vector Magnitude
BER	Bit Error Rate
TWTA	Traveling Wave Tube Amplifier
SSPA	Solid State Power Amplifier
IBO	Input Back-Off
OBO	Output Back-Off
QAM	Quadrature Amplitude Modulation
QPSK	Quadrature Phase Shift Keying

General Introduction

In today's rapidly evolving technological landscape, wireless communication systems have become a cornerstone of modern society, enabling high-speed data transmission, seamless connectivity, and the integration of advanced digital services. The emergence of Fifth Generation (5G) wireless networks marks a significant milestone in this progression, offering unprecedented improvements in terms of data rate, latency, reliability, and massive device connectivity.

Among the key technologies enabling these advancements, Orthogonal Frequency Division Multiplexing (OFDM) stands out as a powerful modulation scheme due to its robustness against multipath fading and its high spectral efficiency. OFDM has thus become a fundamental component of modern wireless communication standards, including 5G.

However, despite its advantages, OFDM suffers from a critical drawback: a high Peak-to-Average Power Ratio (PAPR). This phenomenon can severely degrade the efficiency of power amplifiers, causing signal distortion, increased power consumption, and reduced battery life in mobile devices. Therefore, PAPR reduction has become a major research focus in the design and optimization of OFDM-based systems.

One of the most effective techniques proposed for PAPR reduction is the Partial Transmit Sequence (PTS) method, which works by manipulating phase vectors to minimize the signal peaks. While PTS achieves substantial PAPR reduction, it often suffers from high computational complexity, especially as the number of sub-blocks or phase combinations increases. This complexity presents challenges for practical implementation in real-time and resource-constrained systems.

In this context, the present Master's thesis aims to investigate and evaluate low-complexity variants of the PTS technique for reducing PAPR in OFDM systems tailored for 5G wireless communications. The goal is to develop a solution that balances effective PAPR reduction with minimal computational burden, making it more suitable for practical deployment.

To achieve this objective, we adopted a methodological approach that includes a comprehensive theoretical study, a review of existing techniques, and the design of simulation models using MATLAB. Through these simulations, we analyze and compare the

performance of traditional and improved PTS algorithms in terms of both PAPR reduction and computational complexity.

This thesis is organized into several chapters, each focusing on a specific aspect of the study, including theoretical background, system modeling, simulation results, and concluding insights that highlight the contributions and future research directions.

Chapter Ⅰ

OFDM modulation and PAPR analysis

1.1 Introduction

This chapter is dedicated to the principle of multicarrier modulations, in particular OFDM, and to the characterization of the PAPR of the power OFDM signals. The goal here is to immediately pose the relationship between the PAPR.

OFDM, for Orthogonal Frequency Division Multiplexing [1, 2, and 3] is a method for coding digital signals by distributing them into orthogonal frequencies in the form of multiple subcarriers. The objective is thus to allow good robustness with respect to multipath channels with optimal use of the band due to the fact that the pores overlap each other without interfering because they are orthogonal. This is the most popular and widely used multicarrier modulation technique in telecommunications standards. By way of example, mention may be made of the DAB standard for Digital Audio Braodcasting [4], the DVB-T2 standard (Digital Video Broadcasting-Terrestrial) [5, 6], the WLAN standard for Wireless Local Area Network such as the IEEE 802.11a/g better known under the name Wi-Fi or HYPERLAN [7]. We also find OFDM on the WIMAX or IEEE 802.16 standard or in ADSL for Asymmetric Digital Subscriber Line [8]. Recently, OFDM has also been chosen for the downlink of the LTE standard for Long Term Evolution [9]. Note that in this standard, the single-carrier modulation by SC-FDM packet has been chosen for the uplink and that one of the main causes of this choice is the power consumption due to the fact that these signals are low PAPR while being also robust in the presence of multipath channels.

1.2 Digital transmission chain

Digital transmission systems convey information between a source and a recipient using a physical medium such as cable, optical fiber or even the propagation on a radio channel.

The transported signals can be either directly of digital origin, as in the data networks, be of analog origin (speech, image) but converted under a digital form. The principle of the transmission system is then to convey the information from the source to the recipient with the greatest possible reliability.

The different steps will be explained successively in this chapter. Figure 1.1 summarizes all of these steps in the block diagram of a digital transmission chain.

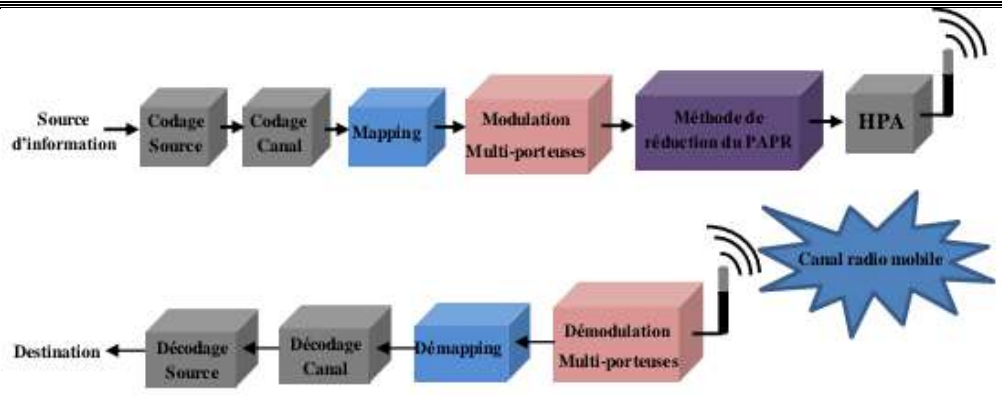

Figure 1.1-Block diagram of a digital transmission chain

1.3 Communication channels

1.3.1 Gaussian white noise channel

The channel model most frequently used for digital transmission simulation, which is also one of the easiest to generate and analyze, is the Gaussian additive white noise channel (BBAG) (Figure 1.2). This noise is generated by parasitic signals passing over the same channel and by the thermal noise of the electronic components. The received signal is written in the form:

$$y(t) = x(t) + b(t), \tag{1.1}$$

Where b represents the BBAG, characterized by a Gaussian random process of zero mean, varianceσ_b^2, and bilateral power spectral density$\frac{N_0}{2}$.

The conditional probability density of y is given by the expression:

$$p\left(\frac{y}{x}\right) = \frac{1}{2\pi\sigma_b^2} e \frac{-(y-x)^2}{\sigma_b^2 2}, \tag{1.2}$$

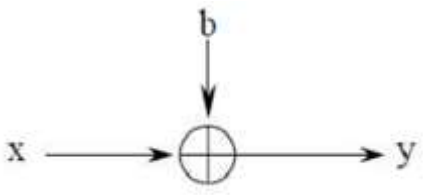

Figure 1.2-Representation of a channel in BBAG.

1.3.2 Multipath channel

This channel is illustrated in Figure 1.7. We consider that the channel undergoes slow fading, that is to say that the duration of a symbol is much less than the coherence time of the channel, and that the signal received therefore does not vary or very little over the duration of a symbol. Taking into account the additive Gaussian white noise, the baseband equivalent signal received at the output of this slow fading channel comprising Np multiple paths is then expressed:

$$y(t) = \sum_{n=0}^{N_p-1} \alpha_n s(t-\tau_n) + b(t), \tag{1.3}$$

Or the complex BBAG noise is represented by $b(t)$, and α_n and τ_n respectively characterize the complex attenuation and the delay affecting each path.

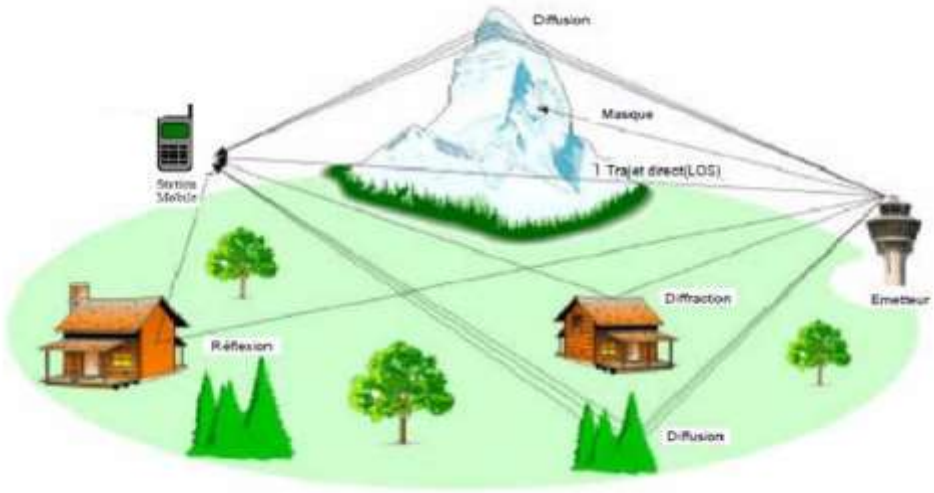

Figure 1.3-Illustration of the phenomenon of multiple paths on the radio-mobile channel.

1.3.3 Propagation channel

Propagation disturbances in digital communications can affect the quality of the received signal. There are several types:

1. Average attenuation: the signal power decreases with distance, in proportion tod^n , where n depends on the environment (2 in direct view, between 3 and 5 in urban or obstructed environments).

2. Multipath propagation: caused by reflections, diffractions and diffusions, it leads to the reception of several phase-shifted and weakened signals, causing frequency selectivity.
3. Doppler effect: due to mobility, it causes rapid variations of the channel in frequency and time, resulting in temporal selectivity.
4. Long-term fading: caused by fixed obstacles (buildings, forests), it leads to attenuations modeled by a log-normal law, affecting the signal in a sustainable way.

1.4 Multi-carrier Modulation

Multi-carrier modulation [10-11] is based on the following principle: during transmission, the frequency-domain signal is transmitted over a certain number N of complex exponentials at different frequencies, called subcarriers. A binary or symbol stream is thus distributed at a rate T_d across all subcarriers, each with a reduced bit rate. Compared to a single-carrier system, the useful transmission duration of a symbol is multiplied by N. This results in a symbol duration $T_s = NT_d$, which ensures that the symbol duration is longer than the maximum channel delay spread, thereby limiting inter-symbol interference. At the receiver, an inverse operation is performed using waveforms matched to those used in transmission.

1.5 Principle of OFDM Modulation

In this section, we will first provide a brief overview of the OFDM, and then we will characterize the PAPR (Peak-to-Average Power Ratio)

1.5.1 OFDM system

OFDM modulation involves transmitting multiple low-rate data streams modulated by carriers that are orthogonal to each other. From a mathematical perspective,

A baseband OFDM signal with M carriers and symbol duration of T_u can be expressed as follows:

$$x(t) = \sum_{n=-\infty}^{+\infty} \sum_{m=0}^{M-1} X_{m,n} g(t - nT_u) e^{j2\pi mFt}, \quad (1.4)$$

With g being a rectangular pulse function of durationT_u, F = 1/T_u represents the spacing between the carriers, mF the m-th carrier frequency, and $X_{m,n}$ the symbol transmitted on the m-th carrier at time nT_u. It is worth noting that the OFDM symbol transmitted at time nT_u is

the sum of the symbols transmitted on the M subcarriers. This OFDM symbol can be expressed as:

$$x_n(t) = -\sum_{m=0}^{M-1} X_{m,n}\, e^{j2\pi mFt}, nT_u \le t \le (n+1)T_u, \quad (1.5)$$

In the following, x_n(t) will denote the OFDM symbol for nT_u≤ t ≤ (n+1)T_u. In the coming chapters we will work more on the symbol than on the signal because the PAPR reduction is done symbol by symbol. In addition, since the PAPR reduction is also done in baseband, unless we specify otherwise, our OFDM symbols will always be defined in baseband. From an analog point of view, an OFDM symbol can be generated via the modulator described in Figure 1.4.

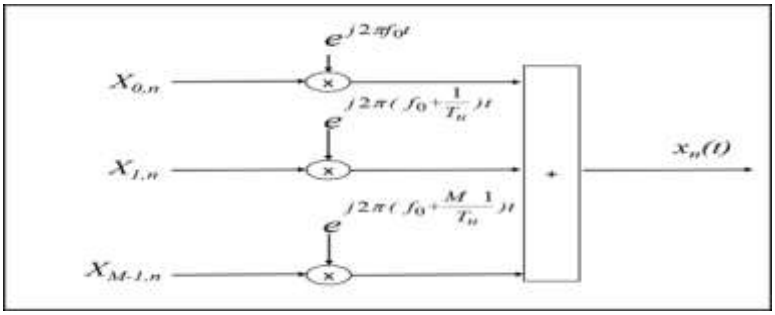

Figure 1.4-Analog modulator of an OFDM symbol

Figure 1.5 shows the spectra of the carriers of an OFDM symbol with M = 4 carriers. Note that the distance between the carriers is$1/T_u$, hence their orthogonality. Indeed, we see that the spectrum of each of the carriers is a cardinal sine and is zero on frequencies that are multiples of $\Delta f = F = 1/T_u$. Due to the orthogonality between the carriers, see Figure 1.2, the demodulation of an OFDM symbol therefore consists of orthogonally projecting the received symbol onto each of the M carriers that it contains. In other words, to recover the information transmitted on the carrier m_0 and at time n0, it is sufficient to apply the matched filtergm_0,n_0(t) = g(t − n_0T_u)e−j2πm0Ft on the received signal y(t) = x(t) ∗ h(t) + n_b(t) where h(t) denotes the impulse response of the transmission channel which will be assumed to be constant throughout the duration of a symbol and n_b(t) an additive noise assumed to be AWGN for Additive White Gaussian Noise. Under the assumption that the channel response around each subcarrier is OFDM Modulation Principle and Characterization of the PAPR of an OFDM signal.

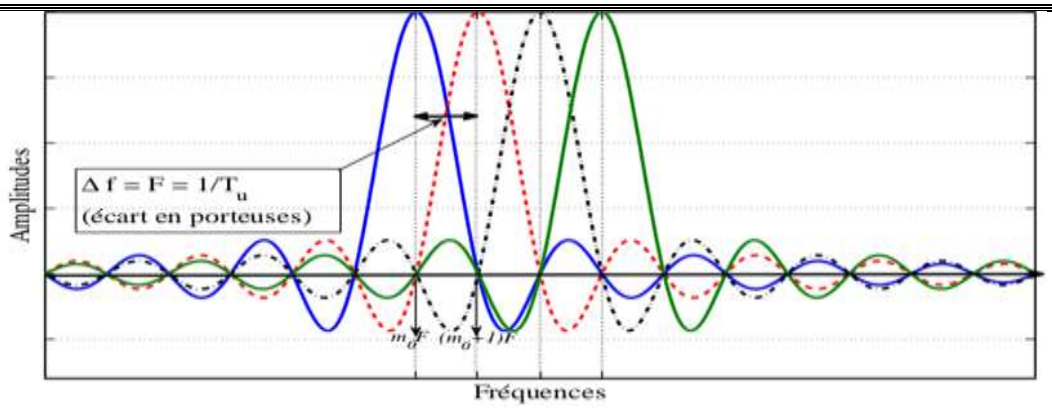

Figure 1.5-Orthogonality between carriers or subcarriers of an OFDM system

Constant, we show after some calculations that:

$$\dot{X}_{m,n} =< y(t), g_{m_0,n_0}(t) >= \frac{1}{T_u}\int y(t)g(t-n_0T_u)e^{-j2\pi m_0 Ft}dt$$

$$= \int_{n_0T_0}^{(n_0+1)T_u} \left(x_n t * h(t)\right)e^{-j2\pi m_0 Ft}dt + n_b[n_0, m_0]$$

$$= \int_{n_0T_0}^{(n_0+1)T_u} \left(\sum_{k=0}^{M-1} X_{k,n}K_k e^{j2\pi kFt}\right)e^{-j2\pi m_0 Ft} + n_b[m_0]$$

$$= H_{m_0}X_{m_0,n_0} + n_b[n_0, m_0] \qquad (1.6)$$

With H_{m_0} the channel response around the m0F carrier and n_b[n0, m0] the noise around the m_0F carrier. Graphically, Figure 1.6 describes the analog demodulator of an OFDM symbol.

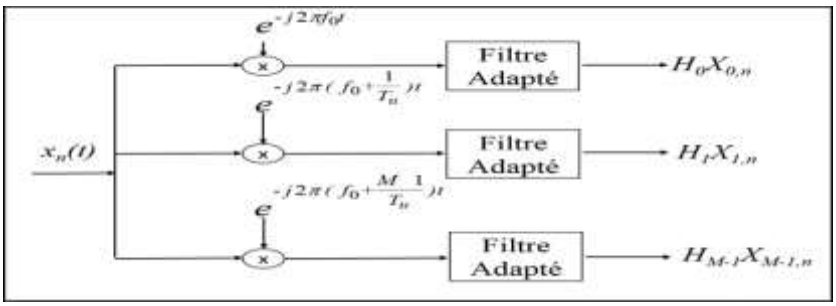

Figure 1.6-Analog demodulator of an OFDM system

1.5.2 Transmitter and Digital Modulator of an OFDM System

In communications, data rates are limited by physical constraints: noise due to imperfections in the electronic components of systems affects the quality of the transmitted signal. Digitizing the data to be transmitted can help improve transmission quality. Digital telecommunications can also enable the use of highly efficient data multiplexing techniques (CDMA for Coding Division Multiple Access), thus allowing optimal use of the bandwidth. In the case of OFDM, it should be noted that implementing the analog modulators and demodulators defined in Figures 1.4 and 1.6 is very complex and resource-intensive. Moreover, the popularity of OFDM began with the invention of the Fast Fourier Transform algorithm, which, as we will see below, enabled an efficient implementation of digital modulators and demodulators for OFDM systems [12].LetT_e=$\frac{T_{Niq}}{L}$ be the oversampling period that we will use to oversample the OFDM signal $x_{(t)}$ defined by (1.4), where T_{Niq}=$\frac{T_u}{M}$ and L ≥ 1 denote the critical sampling period and the oversampling factor, respectively. By denoting $x_{n,l}$ as the sample of $x_{(t)}$ taken at time nT_u+ l$T_e$we have:

$$x_{n,l} = x(nT_u + lT_e) = x_n(lT_e),$$

$$= \sum_{M=0}^{M-1} X_{m,n} e^{i2\pi m \frac{lT_u F}{LM}},$$

$$= \sum_{m=0}^{M-1} X_{m,n} e^{i2\pi \frac{ml}{LM}}, \quad (1.7)$$

In the case of sampling at the critical frequency, it can be observed that:

$$[x_{n,0}, \dots, x_{n,M-1}] = IDFT([X_{0,n}, \dots, X_{M-1,0}]), \quad (1.8)$$

With IDFT standing for Inverse Discrete Fourier Transform. In other words, the discrete OFDM vector x_n = $[x_{n,0}, \dots, x_{n,M-1}]$can be obtained via a Discrete Fourier Transform, which can be efficiently implemented using the FFT (or IFFT) algorithm Fast Fourier Transform or Inverse Fast Fourier Transform.

For more details on the structures of digital modulators and demodulators in OFDM systems, or more generally on multicarrier techniques such as FBMC or oversampled OFDM, the reader may refer to theses [13, 14, and 15]. In what follows, we will now define the digital demodulator of an OFDM system. To do this, let y_n = [$y_{n,l}$, ... , y_{n-M-1})] be the vector containing the samples at the output of the receiver's sampler for the n-th symbol $y_n(t)$.

Assuming that the sampling period is sufficiently small, then equation (1.6) can be approximated as follows:

$$Y_{m,n} = \sum_{l=0}^{M-1} y_{n,l} e^{-j2\pi \frac{ml}{M}} = DFT\left[y_{n,0,\ldots,} y_{n,M-1}\right], \quad (1.9)$$

Recall that $y_n = x_n *$ h, with h being the vector containing the samples of the channel's impulse response. Note that, since the channel is multipath, the most delayed echoes of the previous symbol y_{n-1} can interfere with the current symbol n. Thus, in practice, to address this issue of inter-symbol interference (ISI), a Guard Interval (GI) assumed to be longer than the longest delayed path is added at the beginning of each transmission to contain the echoes of previous symbols.

When the GI is a Cyclic Prefix (CP), meaning it contains the end of each symbol repeated at the beginning, and then equation (1.9) becomes:

$$Y_{m,n} = \sum_{l=0}^{M-1} y_{n,l} e^{-j2\pi \frac{ml}{M} = H_m X_{m,n}}, \quad (1.10)$$

Indeed, the cyclic prefix (CP) transforms the linear convolution of the channel into a circular convolution. Figure 1.4 shows the digital modulators and demodulators of an OFDM system (with M subcarriers).

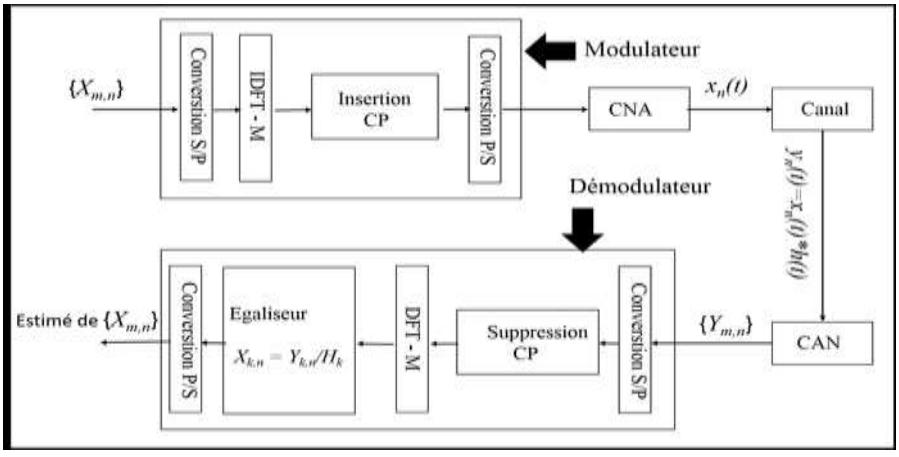

Figure 1.7-Digital Modulator/Demodulator of an OFDM system with Cyclic Prefix (CP)

It is noted that in Figure 1.7, at the transmitter, the cyclic prefix (CP) is placed immediately after the IDFT module and consists of copying the end of each symbol to the beginning. At the receiver, the CP is removed before performing the DFT. Thus, at the cost of a loss in the useful data rate, the cyclic prefix (CP) allows for:

1. Protection against inter-symbol interference (ISI) in OFDM or between OFDM frames.

2. A simple equalizer, as seen in Figure 1.7. The cyclic prefix causes the channel to act on the signal as a circular convolution, which in frequency domain is represented by point-by-point multiplication.

For more details on the construction of the cyclic prefix, its length, etc. In most cases, techniques for reducing the PAPR by adding signals to mitigate the peaks, and thus reduce the PAPR, work at the output of the IDFT before the insertion of the cyclic prefix, as the latter has little effect on the PAPR. We will work with discrete OFDM symbols before inserting the cyclic prefix.

•Advantages and Limitations of OFDM

OFDM modulation is an old technology with recent success that involves transmitting data in parallel on multiple different carrier frequencies. OFDM is particularly well-suited for long-distance radio transmission channels without multiple wave transmission (echoes), significantly reducing inter-symbol interference. However, it can become unusable in the presence of strong echoes, and in such cases, COFDM (Coded OFDM) should be used.

COFDM is a process that combines error correction coding (frequency interleaving) with OFDM modulation. In [16], the author presents the principle of COFDM and the main reasons why it is particularly used in terrestrial broadcasting, mobile networks, etc. In [17], the complexity of the COFDM modulator and demodulator is evaluated, along with the effects of the non-linearity of power amplifiers.

•Advantages of OFDM

•The advantages of OFDM are numerous

• Efficient spectrum usage: Subcarriers overlap while maintaining orthogonality, making better use of frequency resources compared to traditional frequency multiplexing.

• Simplified equalization and decoding: The use of a guard interval and error correction with frequency interleaving (as in COFDM, used in DVB-T) makes the system robust against echoes and multipath effects.

• Resistance to impulsive noise: Since each subcarrier is affected independently, noise impacts only individual symbols, unlike single-carrier systems where one noise event can corrupt multiple symbols.

• Finally, channel estimation in the context of OFDM is simplified by sending training sequences in the frequency domain. The identification of the channel coefficients is done without solving system equations.

•Limitations of OFDM

1.6 OFDM modulation has not only advantages but also disadvantages

• High PAPR (Peak-to-Average Power Ratio): OFDM signals exhibit large amplitude variations after the IFFT, leading to high PAPR. This is problematic for power amplifiers, which must operate in nonlinear regions at high data rates, causing signal distortions like intermodulation and spectral regrowth.

• Sensitivity to frequency offset and synchronization errors:

• Frequency offset disrupts subcarrier orthogonality, leading to intercarrier interference (ICI).

• Synchronization errors cause phase shifts in received symbols.

Traditional correction techniques from single-carrier systems are not effective in OFDM, and new solutions are required especially as higher data rates increase these issues in modern standards.

1.7 Insertion of the Cycle prefix

Disturbances in the propagation channel lead, among other things, to the loss of orthogonality between subcarriers and the appearance of inter-symbol interference (ISI) due to multipath propagation. To eliminate this interference, a simple solution is to increase the number N of subcarriers to extend the symbol durationT_s. However, this approach faces various constraints. The channel coherence time, the Doppler effect, or technological limitations, such as oscillator phase noise, restrict the use of this technique. Another technique can cancel these ISI. Indeed, adding a guard interval of duration T_g, greater than or equal to the maximum delay τ_{Max} of the channel's impulse response, before transmitting the OFDM symbol eliminates this interference. This guard interval is called the "cyclic prefix (CP)." As a

result, the useful T_s of each OFDM symbol is no longer affected by ISI. The total duration T_{tot} of the OFDM symbol is thus increased and becomes $T_s + T_g$. Implementing this technique leads to a loss in spectral efficiency n_g. This loss can be expressed as follows [18]:

$$n(g) = \frac{T_g}{T_g + T_s}, \tag{1.11}$$

The guard interval is inserted at the beginning of the OFDM symbol and is a copy of the end of the same symbol. At the receiver, removing the guard interval restores orthogonality between the subcarriers.

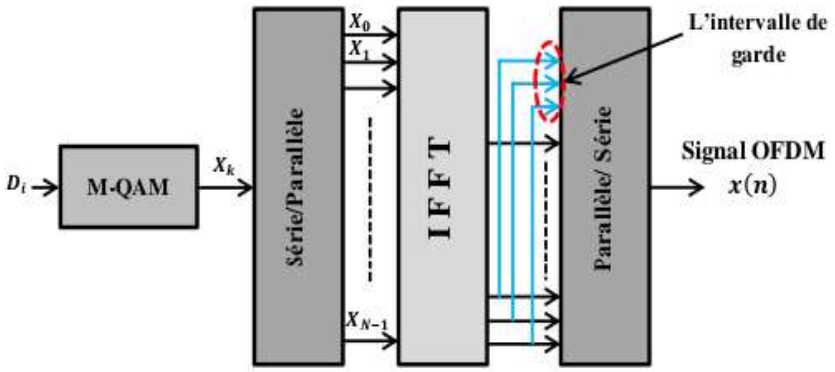

Figure 1.8-Block diagram of CP-OFDM modulation.

Figure 1.9 shows that the spacing between each subcarrier $1/T_s$ ensures that when the spectrum of one subcarrier is at its maximum, the spectra of all others are nullified: this is the condition of orthogonality (Orthogonality of OFDM). This orthogonality condition allows for overlapping spectra of different subcarriers while still avoiding inter-subcarrier interference, provided that sampling is done precisely at the frequency of a subcarrier.

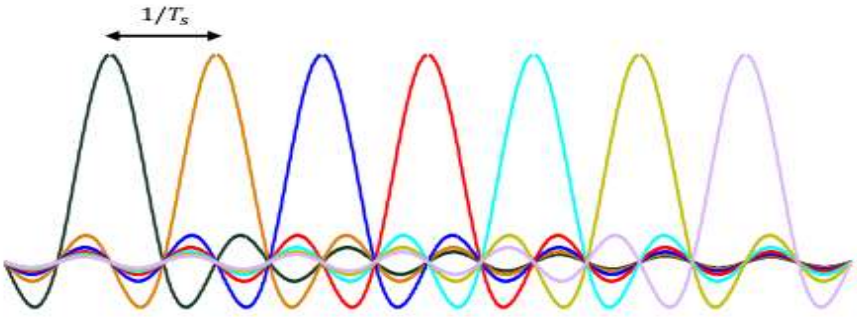

Figure 1.9: Spectra of the different carriers.

1.8 Peak to average power ratio (PAPR) of OFDM Signal

In this section, we will first provide a brief overview of the concept of PAPR. Following this, we will outline the necessary conditions for the oversampling factor of the discrete signal to achieve a good approximation of the PAPR [19] of the continuous signal.

1.8.1. Definition of PAPR

The PAPR [20] is a major parameter in long-distance telecommunication systems. In fact, at the output of the digital-to-analog converter (DAC), it is generally necessary to amplify the power of the signal to be transmitted using a power amplifier [21]. Unfortunately, the power amplifiers non-linear region can cause significant distortion of non-constant envelope signals, such as multi-carrier signals. These distortions are typically difficult to remove at the receiver. Multi-carrier signals exhibit large amplitude variations around the average power. The PAPR parameter is used to measure the temporal dynamics of the signal. Understanding it is essential to characterize the power back-off required to operate the power amplifier without distorting the time-domain signal. It is noted that for signals with high PAPR, such a choice would lead to an oversized amplifier, followed by increased energy consumption, hence the importance of PAPR reduction.

The PAPR describes the power fluctuations of a signal relative to its average power. For a signal x_t defined over a time$[0;\ T_s]$, it is defined as [22, 23]:

$$PAPR_{x_{(t)}} = \frac{\max\limits_{t\in[0;T_S]}\{|x_{(t)}|^2\}}{\frac{1}{T_S}\int_0^{T_S}|x_{(t)}|^2 dt}, \tag{1.12}$$

The PAPR can be applied to analog, digital, finite-support, or infinite-support signals. It has been shown that an upper bound for the PAPR of multi-carrier modulations with N carriers and using symbols from a QAM modulation with carriers and using symbols from a QAM modulation with M states is given by [24]:

$$PAPR_{max,M-QAM} = 3N\frac{\sqrt{M}-1}{\sqrt{M}+1}, \tag{1.13}$$

However, this bound is too broad and does not closely reflect the actual fluctuations of the multi-carrier signal. To address this, we will discuss the characterization of the PAPR of an OFDM signal to obtain a good approximation of the PAPR of the discrete signal.

1.8.2 Characterization of the PAPR of an OFDM Signal

In fact, at the hardware level, PAPR reduction is performed upstream of the digital-to-analog conversion circuit. Therefore, it is important to define an approximation of the PAPR of an OFDM symbol by increasing the oversampling factor. To do this, we will revisit equation (1.8) in a more general context, that is, we will work with oversampling. This choice aims to provide a good approximation of the PAPR of a continuous signal through its discrete samples. It is easy to guess that the larger the oversampling factor, the better the approximation. However, for reasons of numerical complexity, it is interesting to determine up to what value of the oversampling factor **L** we can confidently claim to have a good approximation of the PAPR. Suppose the continuous signal of the OFDM symbol$x_{(t)}$,

Is sampled at a period $T_e = \frac{T_s}{NL}$, we have:

$$x(n) = \sum_{k=0}^{N-1} X_k e^{j2\pi k \frac{n}{NL}}, \qquad 0 \leq n \leq NL-1, \tag{1.14}$$

In digital communication, oversampling is always followed by bandpass filtering to remove spectral replicas at multiple frequencies [25]. We will adopt "Zero-Padding" in the frequency domain to eliminate these replicas. Thus, as in [26], let Ẋ be the vector of dimension NL obtained after the "Zero-Padding" operation on the vector X= $[X_0, X_1, \dots, X_{N-1}]$, that is:

$$\dot{X} = \left[X_0, X_1, \dots, X_{\frac{N}{2}-1}, 0, \dots, 0, X_{\frac{N}{2}}, X_{N-1}\right], \tag{1.15}$$

Then, the discrete symbol vector of dimension NL can still be obtained through an IFFT operation of size NL. The Complementary Cumulative Distribution Function (CCDF) is the most commonly used tool in the literature to characterize the necessary back-off that allows signal amplification without distortion. Indeed, as its name suggests, the CCDF is the probability that the PAPR of the OFDM symbol exceeds a threshold represented by$PAPR_0$. We have:

$$CCDF(PAPR_0) = prob(PAPR_{X_{(n)}} > PAPR_0), \tag{1.16}$$

1.9 Conclusion

This chapter provided a comprehensive overview of the structure and evolution of modern telecommunications networks, focusing particularly on the advancements and challenges in fifth-generation (5G) wireless systems. It began with the evolution of mobile networks, from earlier generations to high-speed 5G, followed by an analysis of the protocol layers ensuring efficient data transmission. A significant section was devoted to understanding the mobile radio channel through both physical and statistical models, essential for robust wireless system design. The chapter also examined multi-carrier modulation, especially Orthogonal Frequency Division Multiplexing (OFDM), highlighting its role in enhancing spectral efficiency and mitigating multipath effects. A critical issue discussed was the Peak-to-Average Power Ratio (PAPR) in OFDM, which impacts amplifier efficiency. By introducing and analyzing PAPR, the chapter lays the groundwork for the advanced reduction techniques that will be explored in the following sections, establishing a foundation for optimizing performance in 5G and beyond.

Chapter Ⅱ

The High Power Amplifier (HPA)

2.1 Introduction

In digitized telecommunication systems, transmitters use power amplifiers to efficiently transmit the RF signal, compensating for losses due to propagation. These amplifiers, essential but energy-intensive, must operate in non-linear zones to maximize efficiency, which causes distortions accentuated by a high PAPR (peak amplitude ratio). This sometimes forces the amplifier to be oversized, reducing energy efficiency. This chapter analyzes the characteristics of power amplifiers in a digital context, their behavioral modeling, as well as indicators such as ACPR, SNR, EVM and intermodulation products. It concludes with a study of the effects of non-linearities on spectral density and BER in digital systems.

2. 2 Power Amplifiers Overview

2.2.1 Definition

To ensure reliable signal transmission, power amplifiers boost the radio frequency signal to prevent degradation during propagation. They draw energy from a DC power supply and are generally classified into two main categories used in communication systems [27]:

- Travelling Wave Tube Amplifier (TWTA) [28] a vacuum tube used at microwave frequencies to build wideband amplifiers with low noise, suitable for low to high power levels. It is especially used in satellite communication systems.
- Solid State Power Amplifier (SSPA) [29] an electronic device that amplifies electrical signals by increasing their voltage and/or current, using energy from a power supply. It is commonly used in terrestrial radio transmissions, such as mobile phones and radio loops.

2.2.2 Characterization of the Power Amplifier: AM/AM and AM/PM Conversions

To determine the relationship between the input power, the power consumed by the amplifier, and the output power of the signal, we will consider the graph below, which shows the input-output relationship (AM/AM for Amplitude/Amplitude), referred to as transfer characteristics or AM/AM transfer function [30].

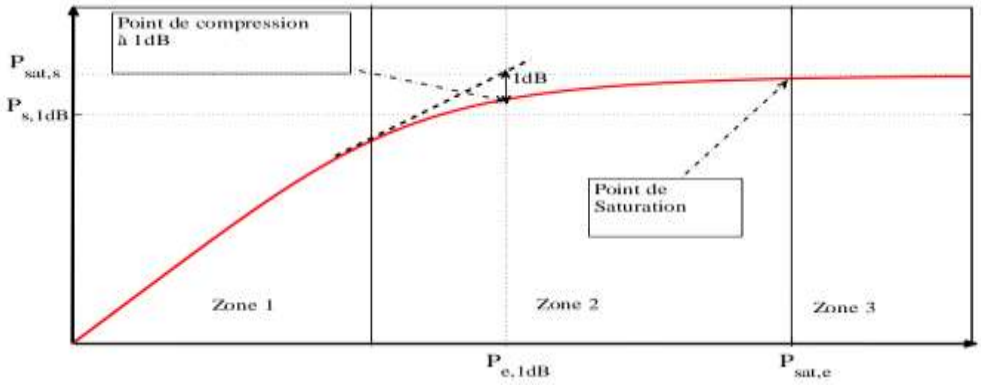

Figure 2.1-Shape of the AM/AM Curve of a Power Amplifier.

Operating Regions of a Power Amplifier (Based on AM/AM Curve) [31]:

1. Zone I – Linear Region: Output is proportional to input with constant gain and minimal distortion, but efficiency is low due to amplifier oversizing.
2. Zone II – Compression Region: Begins to show non-linear behavior, causing increasing signal distortion especially problematic with high PAPR signals like those in multicarrier systems.
3. Zone III – Saturation Region: Output power no longer increases with input; maximum distortion occurs, significantly degrading signal quality.

2.3 Key Parameters of the Power Amplifier

2.3.1. Power Efficiency

The power amplifier boosts a baseband signal to a level suitable for transmission, using energy from a DC power source. The input powers include the DC power and the input signal power, while the output powers consist of the RF output power and the power lost as heat (Joule effect). These powers are related by an energy balance equation [32]:

$$p_e + p_{dc} = p_s + p_{diss}, \tag{2.1}$$

Unfortunately, in reality, it must also be considered as pure loss power dissipated within the amplifier, as shown in the power balance diagram of Figure 2.2.

Power efficiency refers to a measure of how much of the DC power p_{dc} is effectively converted into useful output power p_s The criteria for power efficiency provide insight into the power losses p_{diss} , which is an extremely important aspect in the design and sizing of heat dissipation or cooling systems. Among the various measures of energy efficiency, the most common one is the DC efficiencyη_{DC}, defined as the ratio between the power p_s

delivered to the load the antenna, in this case and the power consumption p_{dc} of the amplifier:

$$\eta_{DC} = \frac{p_s}{p_{dc}}, \tag{2.2}$$

Other measures [31, 32] of the essential criterion for evaluating the performance of power amplifiers are the efficiency ρ_p defined by equation (2.3), and the Power Added Efficiency (PAE), defined by equation (2.4):

$$\rho_p = \frac{p_s}{p_e + p_{dc}}, \tag{2.3}$$

$$PAE = \frac{p_s - p_e}{p_{dc}}, \tag{2.4}$$

These measures provide an idea of both efficiency and gain simultaneously, unlike energy efficiency.η_{DC}

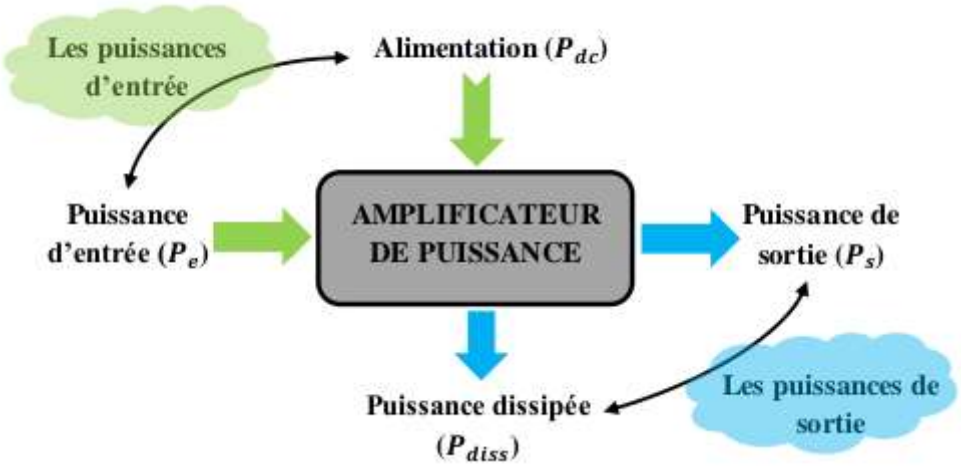

Figure 2.2-Simplified Power Balance of a Power Amplifier.

2.3.2 Input Back-Off and Output Back-Off

A signal passing through a power amplifier then experiences both AM/AM compression. It is necessary to introduce the concepts of Input Back-Off (IBO) and Output Back-Off (OBO), which represent the input back-off and output back-off, respectively. Let$p_{e,1dB}$ and $p_{s,1dB}$ be the respective input and output powers at the 1dB compression point. The IBO, typically expressed in dB, is the ratio between the saturation power adjusted to the input (or the input power at the 1dB compression point) and the input power of the signal:

$$IBO = 10log_{10}\left(\frac{p_{e,sat}}{p_e}\right)[dB]\,, \tag{2.5}$$

Or alternatively [33]:

$$IBO = 10log_{10}\left(\frac{p_{e,1dB}}{p_e}\right)[dB]\,, \tag{2.6}$$

In the same way, the OBO parameter is defined as the ratio between the saturation power (or the output power at the 1dB compression point) and the average output power of the signal:

$$OBO = 10log_{10}\left(\frac{p_{s,sat}}{p_s}\right),[dB]\,, \tag{2.7}$$

Or it can be written as follows [33]:

$$OBO = 10log_{10}\left(\frac{p_{s,1dB}}{p_s}\right),[dB]\,, \tag{2.8}$$

• The greater the IBO, the closer the amplifier is to its linear region, and thus it is oversized.

• The higher the PAPR of the input signal, the higher the IBO required to operate the amplifier in its linear region.

• The OBO gives the power loss associated with each value of the IBO.

Figure 2.3 shows the AM/AM curve as well as the curve (shape) of the power amplifier's energy efficiency.

From Figure 2.3, we can observe that oversizing the power amplifier results in inefficient operation in terms of energy consumption. Indeed, it is noted that the larger the power back-off (IBO), the more the amplifier operates in its linear region (Zone 1), which is the region where the amplifier's efficiency is low. It is also noted that Zone 2 (especially the operating point at 1dB) serves as a buffer zone, allowing a trade-off between energy efficiency and signal degradation.

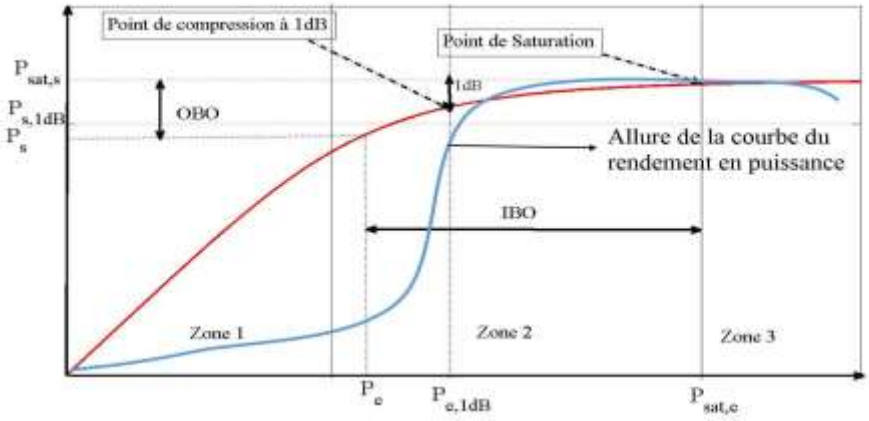

Figure 2.3-Key Parameters of a Power Amplifier

2.4 Operating Classes of the Power Amplifier

The definitions of the operating classes of the amplifier apply regardless of the semiconductor technology used for the amplifier design [34-35], but rather in relation to the conduction angle 2θ of the drain current [36]. There are many operating classes for power amplifiers. Amplifiers are classified into classes A, B, AB, and C for analog amplifiers, and D, E, and F for switching amplifiers. The most commonly used amplifier classes are A, B, AB, and C.

1. The class (A) amplifier has a linear characteristic, and the amplified signals undergo low distortion at the cost of low efficiency. In fact, the maximum theoretical efficiency of an amplifier in this class is 50%, but due to the linearity requirements of applications, the efficiency is typically limited to 25%.Its conduction angle is $2\theta = 2\pi$
2. The class (B) amplifier is generally used for applications that do not have strict linearity requirements. The efficiency of a class (B) amplifier is significantly better than that of a class (A) amplifier, reaching 78% [89, 90], while still providing a certain level of linearity. It has a conduction angle of $2\theta = \pi$
3. In a class (AB) amplifier, the conduction angle 2θ is between π and. 2π the class (AB) amplifier is a compromise between class (A) and class (B). The distortion of a class (AB) amplifier is higher than that of a class (A) amplifier, but lower than that of a class (B) amplifier. On the other hand, a class (AB) amplifier has an efficiency that is lower than the theoretical maximum efficiency of class (B), but higher than that of class (A), meaning its efficiency is between 50% and 78%. The class (AB) amplifier is, in general, the most commonly used.

4. The class (C) amplifier, whose conduction angle 2θ is less than π has a very pronounced non-linear characteristic. This result in significant distortion in the amplified signal, making it unsuitable for applications that require a high level of linearity. Class (C) amplifiers have an efficiency close to 100%. Table 2.1, extracted from [37], summarizes the various characteristics of analog power amplifier classes.

Table 2.1-Characterization of the Operating Classes of Power Amplifiers.

Classe	Angle de conduction (2θ)	Puissance de sortie	Rendement maximal	Gain	Plage de linéarité
A	2π	Satisfaisante	50%	Important	Grande
B	π	Moyenne	78.5%	Moyen	Moyenne
AB	Entre π et 2π	Moyenne	50% à 78.5%	Satisfaisant	Satisfaisante
C	Inférieur à π	Faible	100%	Faible	Faible

2.5 Behavioral Modeling of an Amplifier

2.5.1 Saleh Model

The most common model for traveling wave amplifiers is the Saleh model [28], whose AM/AM and AM/PM transfer characteristics are given below:

$$\mathcal{F}_A[A(t)] = \frac{\alpha_a[A(t)]}{1+\beta_a[A(t)]^2}, \qquad \mathcal{F}_\emptyset[A(t)] = \frac{\alpha_\emptyset[A(t)]^2}{1+\beta_\emptyset[A(t)]^2}, \tag{2.9}$$

Note that for large values of the amplitude$A(t)$,$\mathcal{F}_A[A(t)]$ is proportional to$1/A(t)$, and $\mathcal{F}_\emptyset[A(t)]$ approaches a constant. In [28], the values of the parameters$\alpha_a, \beta_a, \alpha_\emptyset \ and \ \beta_\emptyset$ are obtained through experimental measurements in a multicarrier transmission framework and are given by:

$$\alpha_a = 1.9638, \beta_a = 0.9945, \alpha_\emptyset = 2.5293, \beta_\emptyset = 2.8168\,, \tag{2.10}$$

2.5.2 Rapp Model

The commonly used model for semiconductor amplifiers in multi-carrier transmissions is as follows [29]:

$$\mathcal{F}_A[A(t)] = \frac{G.A_{(t)}}{[1+[\frac{A_{(t)}}{A_0}]^{2\rho}]^{\frac{1}{2\rho}}}, \qquad \mathcal{F}_{\emptyset}[A_{(t)}] \approx 0, \tag{2.11}$$

Where is the amplitude of the saturation output voltage, the power gain of the amplifier and ρ is a factor often called "Smoothness Factor" in English, which allows to control the transition between the linear region and the saturation region of the AM/AM transfer characteristic of the amplifier.

2.6 Measurement of Distortions

This section is dedicated to the general definitions of quality measures in transmission that allow for an objective evaluation of the linearity of a transmitter. Measurements in the frequency domain will assess the power of intermodulation products in the vicinity of the useful band, and here we will focus on measuring the Adjacent Channel Power Ratio (ACPR). In the time domain, the fidelity of the transmitted signal can be evaluated by the magnitude of the error vector (EVM for Error Vector Magnitude), as shown below.

2.6.1 Adjacent Channel Power Ratio (ACPR)

To quantify the interference generated in the adjacent bands of the useful band, an ACPR parameter is defined. The ACPR [37] is defined by the power difference between the main lobe (useful band) and the secondary lobes, as shown in Figure 2.3. We speak of right ACPR and left ACPR, depending on the side of the adjacent band considered. The ACPR is given by the following relation:

$$ACPR = \frac{\int_{BU} DSP(f)df}{\int_{BA} DSP(f)df}, \tag{2.12}$$

Where BU and BA represent the useful band and the adjacent band, respectively.

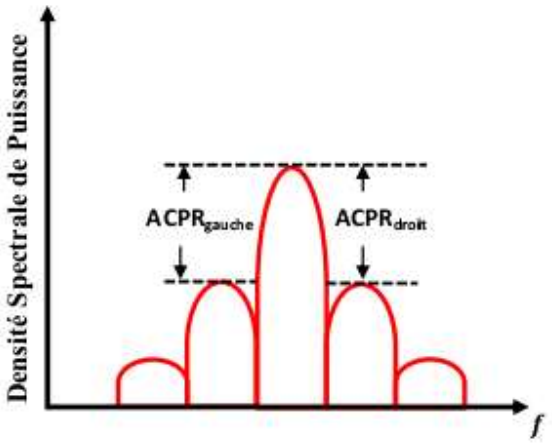

Figure 2.4-Calculation of ACPR.

2.6.2 Error Vector Magnitude (EVM)

In the time domain, radio transmission involves variations in amplitude and phase around the main carrier, expressed as complex pairs (I and Q components). Nonlinearities in the amplifier degrade the signal, causing errors in the recovered I and Q components during reception, leading to increased Bit Error Rate (BER). The transmission channel itself introduces further degradations like attenuation, echoes, fading, and interference. To ensure optimal signal quality, the Error Vector Magnitude (EVM) can be calculated at each symbol time, helping to evaluate signal integrity from the point of emission.

Let X_n be the complex time signal (emitted) measured in reception or in transmission and let $\dot{X}_n$ be the ideal reference signal. The EVM is calculated as follows:

$$EVM = \sqrt{\frac{\sum|X_n - \dot{X}_n|^2}{\sum|X_n|^2}}, \tag{2.13}$$

Figure 2.4 shows how to calculate the EVM.

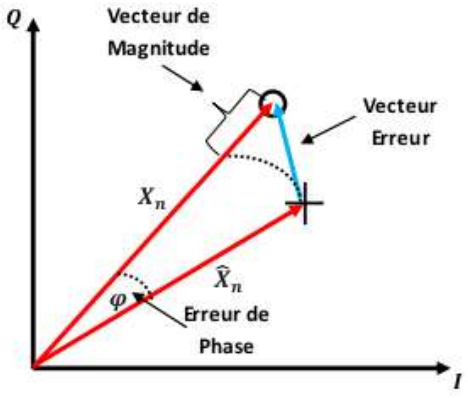

Figure 2.5-Calculation of the EVM.

2.7 Effect of power amplifier on communications systems

The non-linearity of the power amplifier would not be a problem if the input signals were of constant envelope and low dynamic range (low PAPR). This is the case, for example, in GSM signals. Future communication systems (4G or 5G) will have to face the existing problem of the non-linearity of the power amplifier but with an additional difficulty, due to the specific nature of the signals (multi-standard signals, therefore very wide and with very high dynamic range, i.e. high PAPR). We present in the following, the distortions caused by the non-linearity of the power amplifier and the consequences on the quality of the transmission. We use a communication system which integrates a Rapp amplifier [29] whose AM/AM and AM/PM transfer characteristics are given by equation (2.11). To efficiently use the available spectrum, current digital transmission systems use multi-carrier modulations with a large number of phase states and amplitudes. However, these modulations are very sensitive to distortions, of course, non-linear distortions coming from the amplifiers in the transmission chain.

The amplifier has a direct impact on the constellation, which results in a deformation of the constellation, thus causing errors in the transmitted bits (see Figure 2.5). To illustrate this phenomenon, we consider a simplified diagram consisting of an input signal (from a 16-QAM modulation) and an SSPA type power amplifier (given by the Rapp model). A white Gaussian noise W(t) is added to the amplifier output.

The signal $x_{(t)}$ at the input of the power amplifier is a monostandard WLAN type signal (OFDM signal of N=64 subcarriers, 16-QAM modulation). The EVM calculated from the signals $x_{(t)}$ and $y_{(t)}$ is given by Figure 2.6. It shows that the EVM decreases when the input recoil increases, that is, when the amplification is increasingly in the linear zone. It also shows that the EVM decreases with the signal-to-noise ratio (SNR). Indeed, a low IBO generates significant distortions in the amplified signal; in the same way, a low SNR means a fairly high noise level in the band that will significantly disturb the transmitted signal.

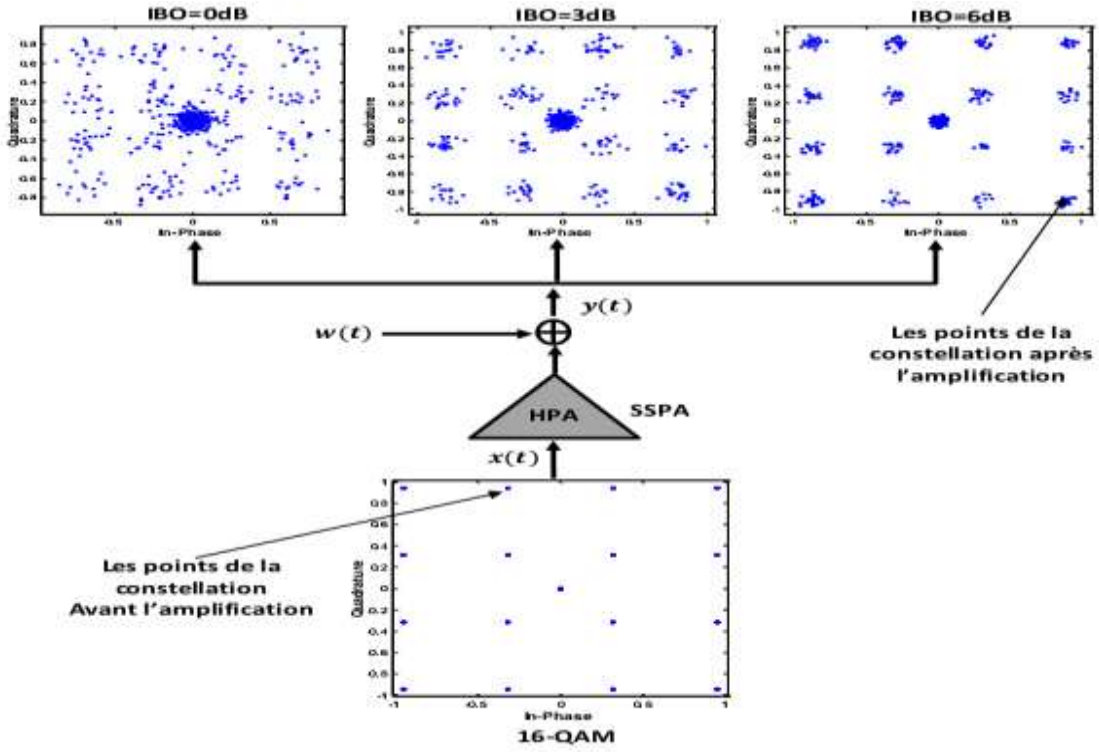

Figure 2.6-Effect of the power amplifier on the constellation points.

2.7.1 Effect on the spectrum

The influence of the non-linear characteristic of the amplifier on the amplified signals is also expressed by spectral lift. This results in interference with other signals emitted in neighboring channels. The figure of merit that allows us to measure interference with adjacent channels is the ACPR which was defined in equation (2.12). Table 2.2 shows the ACPR measurements according to the IBO values, where BU = BA = 5 MHz, it will be a question of showing the influence of a non-linear amplification on the spectrum of signals with high dynamics (high PAPR). The phenomenon of spectral lift is shown in Figure 2.7. It shows that the spectral lift (interference with adjacent channels) increases when the recoil decreases. Indeed, low values of the IBO mean that the power amplifier is operating at the limit of its saturation zone. It is in this area that the signals undergo the most distortion, which explains the increasingly significant spectral rise when the IBO becomes increasingly weak.

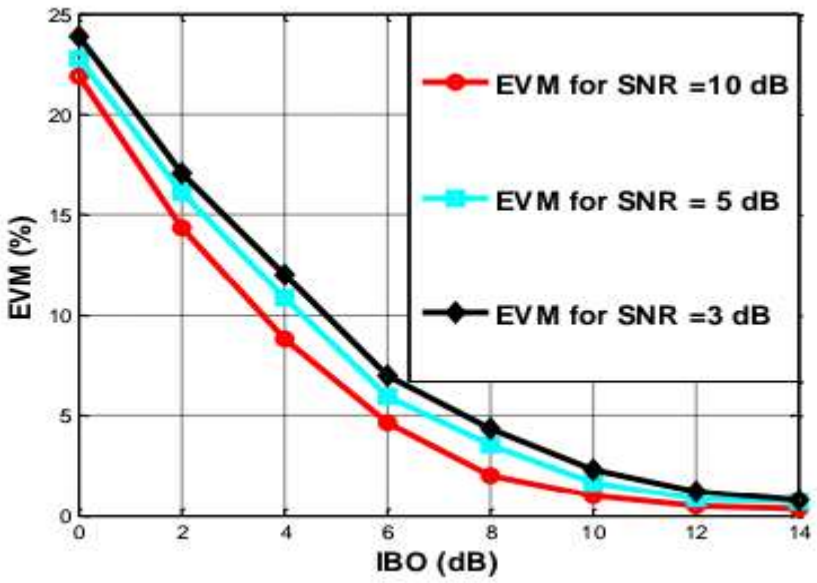

Figure 2.7-EVM as a function of input backoff (IBO) for different SNR values.

2.7.2 Effect on the bit error rate

We have seen that a non-linear amplification of the signals has a direct impact on the constellation which results in an EVM which increases with the loss of linearity (when approaching the saturation zone). This inevitably has an impact on the BER. Figure 2.8 gives the BER performance as a function of the SNR for different input backoff (IBO) values. The simulated transmission system is of the OFDM type comprising 64 16-QAM modulation subcarriers. The transmission channel is a Gaussian channel as shown in Figure 2.5. We can indeed observe a degradation of the BER performance for low IBO values. However, when the IBO becomes significant, the BER tends to merge into the OFDM curve without HPA.

This is proof that there are fewer disturbances related to amplifier non-linearities when the signal is amplified in the linear zone and when the signal is amplified more and more in the saturation zone; it undergoes more and more distortions.

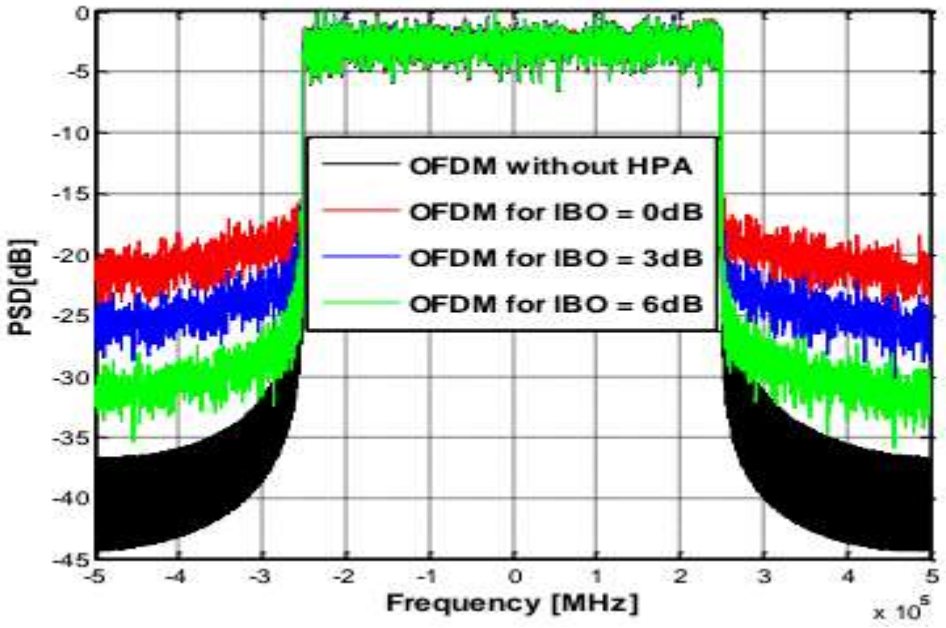

Figure 2.8-Effect of the power amplifier on the spectrum for different values of IBO.

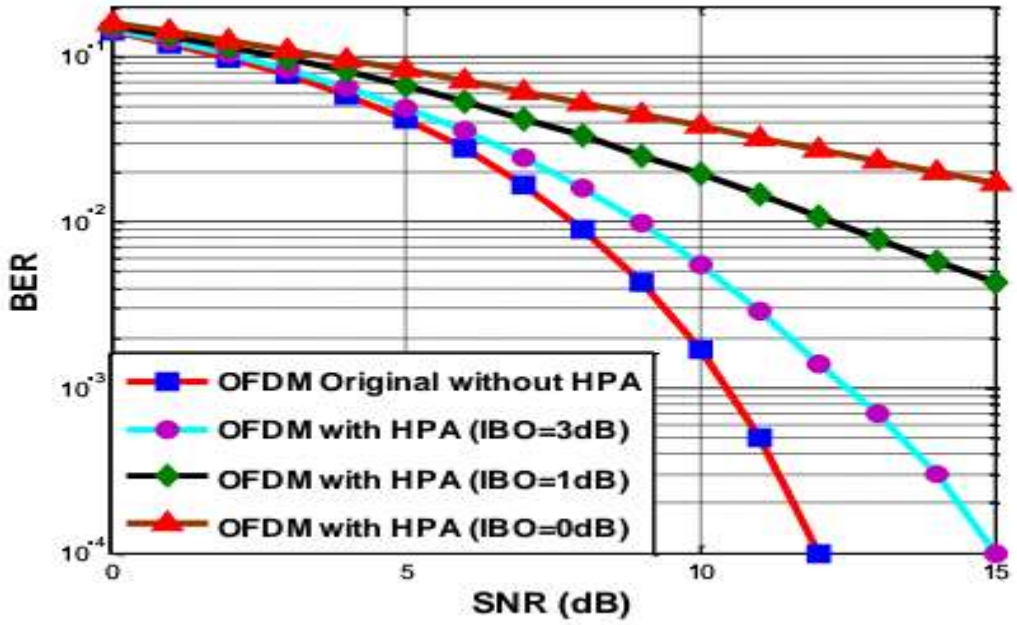

Figure 2.9-Effect of power amplifier on BER for different IBO values.

Table 2.2-Example of ACPR measurement according to IBO values.

IBO (dB)	*0*	*3*	*6*	*12*	*15*
ACPR (dB)	*-34,1210*	*-34,0124*	*-33,8102*	*-33,4342*	*-33,2178*

2.8 Conclusion

In this chapter, we thoroughly examined the role of power amplifiers in OFDM systems, starting with their basic definitions and efficiency-related parameters such as power efficiency and input/output back-off. We explored how these factors influence performance in multicarrier environments, along with the different amplifier operating classes and the detrimental impact of nonlinearities on signal integrity. To analyze these effects, behavioral models like Saleh and Rapp were introduced. We also presented essential distortion metrics such as Adjacent Channel Power Ratio (ACPR) and Error Vector Magnitude (EVM), which are crucial for evaluating amplifier performance. The chapter concluded by emphasizing the significant influence of power amplifiers on spectral behavior and bit error rate (BER), especially in modern wireless communications like 5G. Overall, this chapter provides a foundation for understanding the interaction between analog amplification and digital system performance, paving the way for upcoming chapters on mitigation techniques such as PAPR reduction.

Chapter Ⅲ

Low Complexity PTS for PAPR Reduction

3.1 Introduction

Orthogonal Frequency Division Multiplexing (OFDM) is a widely adopted modulation technique in modern wireless communication systems, including 5G networks, due to its high spectral efficiency and robustness against multipath fading [38]. However, a major drawback of OFDM is its inherently high Peak-to-Average Power Ratio (PAPR), which can severely degrade the performance of power amplifiers, leading to power inefficiency and signal distortion [39].

To address this issue, various PAPR reduction techniques have been developed. Among them, the Partial Transmit Sequence (PTS) technique is a prominent distortionless method that can effectively reduce PAPR without compromising the bit error rate [40]. Despite its effectiveness, the conventional implementation of PTS suffers from high computational complexity, especially when a large number of sub-blocks and phase rotation factors are used [41].

In the context of 5G wireless systems, where low-latency and energy efficiency are crucial, it is essential to optimize the PTS algorithm to reduce its complexity while maintaining acceptable PAPR reduction performance. This chapter presents a detailed discussion of the conventional PTS technique, analyzes its computational complexity, and introduces a proposed low-complexity variant. A theoretical comparison is also provided to evaluate the trade-offs between complexity and performance.

3.2 Conventional PTS Technique

Orthogonal Frequency Division Multiplexing (OFDM) is a highly efficient multicarrier modulation scheme, widely adopted in 5G and other modern wireless systems due to its robustness against multipath fading and high spectral efficiency. However, one of the critical challenges of OFDM is the **Peak-to-Average Power Ratio (PAPR)** problem. Among the various techniques proposed to mitigate PAPR, the **Partial Transmit Sequence (PTS)** method is considered one of the most effective distortionless schemes [42].

3.2.1 Principle of PTS

The PTS technique works by dividing an input OFDM symbol (in the frequency domain) into multiple disjoint sub-blocks. These sub-blocks are individually multiplied by a set of phase rotation factors, and then combined to form a time-domain OFDM symbol with lower

PAPR. The goal is to find the optimal combination of phase factors that minimizes the PAPR of the resulting OFDM signal.

Let the input frequency-domain data block be denoted as:

$$X= \{X_0, X_1, X_{N-1}\}, \tag{3.1}$$

This block is divided into V disjoint sub-blocks:

$$X= \sum_{v=1}^{V} X_v, \tag{3.2}$$

Each sub-block X_v contains non-zero elements only in a specific portion of the total spectrum, and zeros elsewhere. Each sub-block is then multiplied by a phase factor∋ $b_v B$, where B is a predefined set of allowed phase values (e.g., B= {j, −j, 1, −1}

The combined signal becomes:

$$X'=\sum_{v=1}^{V} X_v b_v, \tag{3.3}$$

An IFFT is then applied to X′ to obtain the time-domain OFDM symbol:

$$x'=(\sum_{v=1}^{V} X_v b_v)\text{IFFT}, \tag{3.4}$$

The combination $\{b_1, b_2, \dots, b_V\}$ that results in the lowest PAPR is selected for transmission.

3.2.2 PTS Sub-block Partitioning Methods

There are several methods for partitioning the input data block into sub-blocks:

- **Adjacent Partitioning**: Consecutive subcarriers are grouped into sub-blocks.
- **Interleaved Partitioning**: Subcarriers are assigned to sub-blocks in a periodic pattern.
- **Pseudo-random Partitioning**: Subcarriers are assigned based on a pseudo-random sequence.

The choice of partitioning affects both performance and complexity [43].

3.2.3 Search Complexity

For each possible combination of phase factors, an IFFT operation is required to compute the resulting PAPR. If W phase factors are used per sub-block, then W^{V-1}combinations must be checked (since one phase can be fixed to avoid ambiguity). This leads to **exponential**

growth in computational complexity, which is a major drawback of the conventional PTS method, especially when a high number of sub-blocks is used.

3.3 Partial Transmission Sequence Method

Among the most studied techniques for PAPR reduction is PTS, as both offer a significant reduction in PAPR. Furthermore, PTS allows the use of metheuristic strategies for reduced computational efficiency. Specifically, in a PTS, the insight transmission is typically divided into disjoint sub-blocks. The IFFT block is typically used, and then the sub-blocks are rotated and balanced using a weight vector. The sub-blocks are then summed, and the transmission PAPR is definitively determined for each step vector. This process is typically repeated until the preferred PAPR is definitively discovered.

3.3.1. PTS technique for PAPR reduction of OFDM signal

The idea of this method [44] is to truncate the N train of carriers into V blocks of N/V carriers. A carrier used in a particular block will be set to zero in all the others. Once these N/V blocks have been formed, the initial idea of the SLM technique is applied; a vector$b_{v=e^{j\frac{2\pi}{w}\gamma_v}}, \gamma_v \in \{0,\dots,w-1\}\, et\ v = 0,1,\dots,v-1$, will perform a weighting of each of the V blocks after IFFT to form the final signal at the weakest PAPR. As illustrated in Figures 3.3 and 3.4, the PTS algorithm is as follows:

(i) The frequency OFDM symbol X of N carriers is truncated into V disjoint sub-blocks X^v of N/V carriers such that; X=$\sum_{v=0}^{V-1} X^v$

(ii) Each disjoint sub-blockX^v, a phase shift is applied and the new frequency OFDM symbol is written:

$$X_b=\sum_{v=0}^{V-1} b_v X^v, \tag{3.5}$$

(iii) The temporal OFDM symbol $x_b(n)$ is then written:

$$x_b(n)=\text{IFFT}\{\sum_{v=0}^{V-1} b_v X^v\}=\sum_{v=0}^{v-1} b_v\, IFFT\{X^v\}=\sum_{v=0}^{V-1} b_v X^v(\text{n}), \tag{3.6}$$

Where the phase shift vector b_v is optimized as follows:

$$\hat{\text{b}}=\underset{b_v}{argmin}\left(\underset{0 \le n \le N.L-1}{max|x_b(n)|}\right),$$

The transmission signal is given by:

$$x_{\hat{b}}(n)=\sum_{v=0}^{V-1} \hat{b}_v X^v(n), \quad (3.7)$$

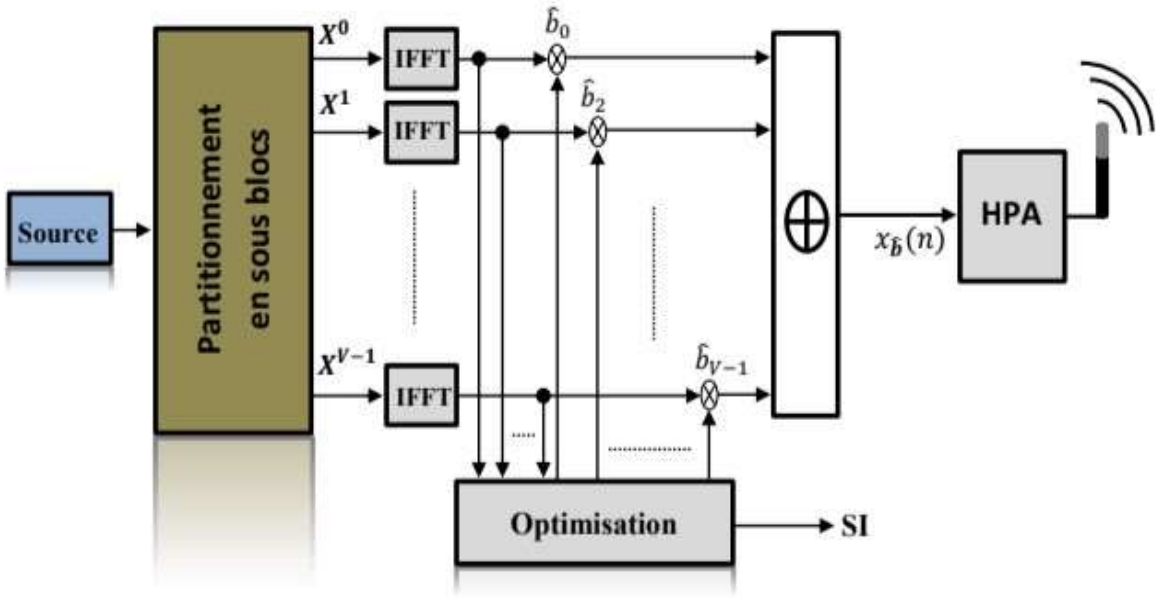

Figure 3.1-Schematic diagram of the PTS.

The way the symbols are partitioned into sub-blocks has an influence on the performance and complexity of the technique. The major drawback of the PTS technique lies in the complexity of the search for $b_v$weighting vectors to minimize the PAPR. Indeed, considering V sub-blocks and binary weighting factors (the vectors b_v, v =1,2 are only composed of 1 or -1), the number of possible combinations is v which must all be reviewed to determine the set of vectors that minimizes the PAPR. Another disadvantage of the PTS technique is that it requires the transmission of information lateral (SI) so that the receiver identifies the sequence that made it possible to generate the lowest PAPR.

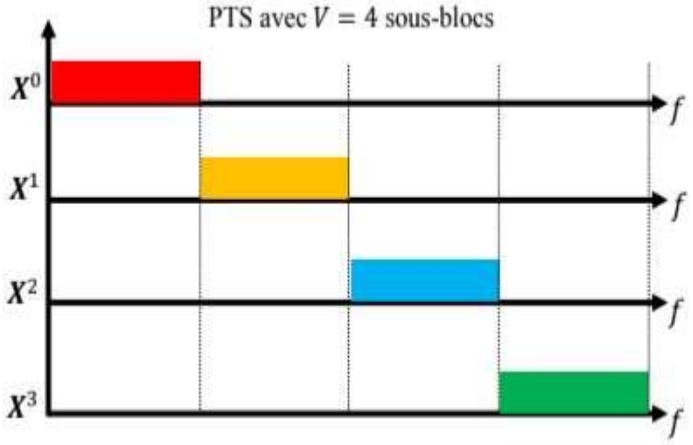

Figure 3.2-Example of partitioning a symbol into sub-blocks for the application of the technical PTS.

The standard PTS system requires a thorough search to find the optimal vector, which leads to great computational complexity, which can be the main disadvantage of this system. To get rid of this disadvantage of the PTS, many probabilistic strategies are launched in the following literature:

- As in the I-PTS technique (Iterative Flipping Algorithm) [45], the first step is the calculation of the POPE of the original signal, then the second step begins with the multiplication of the second sub-block by the factor$b_1 = e^{j\frac{2\pi}{w}\gamma_1}$, then the calculation of the PAPR each time and finally the extraction of γ'_1 which corresponds to the lowest of the PAPR values. This value is kept in this sub-block, knowing that the first sub-block is multiplied by the factor $b_0 = 1$ and that this operation continues until the last step. If the number of search processes is W. Therefore, the complexity of the search for this technique is proportional to W (V-1).
- In the GD-PTS (Gradient Descent) technique [46], initially, all the factors of they consider that$b_v = 1$,v =0,...,v-1. Then, GD-PTS optimizes the phase factors iteratively with respect to their previous phase factors. The phase factors eligible for optimization are those for which the Hamming distance is equal to or substantially less than the radius r of their origin. Which means that the computational complexity of the GD-PTS is proportional to$C_r^{V-1}.W^r$. I, or I is the maximum number of iterations and C_r^{V-1} $=\frac{(V-1)!}{r!(V-1-r)!}$ is the binomial coefficient.

- ABC-PTS (Artificial Bee Colony) was proposed by Karaboga [47]. In this algorithm; the bees used, the observer bees and the scout bees have the task of obtaining optimal food resources. In the first place, the positions food resources are produced randomly. In the problem of decreasing the value of the PAPR, the placement of a food source is identical to the phase vector $b_i = [b_{i0}, b_{i1}, \dots, b_{i(V-1)}]$ or i=1,...,SN and SN where and indicates the size of the population, which includes the bees used or the observer bees. The bees used are looking for a fresh food source in a radius close to the previous resource, if the amount of nectar from the new resource is greater than the previous one. The new offer is remembered as an optimal answer. The steps of the ABC algorithm [10] are repeated within a cycle called the maximum cycle (MC). In a cycle, the possible solutions food numbers (FN) are identified and, in the ABC-PTS algorithm, possible solutions MCN× FN are suggested to obtain the optimal phase vector.
- The BFO-PTS technique (Bacteria Foraging Optimization) which models the feeding behavior of E-coli bacteria has been presented and developed by Passino [48]. BFO is a complex algorithm composed of three steps organized in nested loops: (i) the stage of chemotaxis: it models the way in which the bacteria move in the degraded nutrients. It consists of two parts: tumbling and swimming. A fall is simply a reorientation of the bacteria in a random direction. A swim is a movement of the bacterium in the direction of the tumble of a specific step for every bacterium. (ii) The reproduction stage: the bacteria are sorted by health, the unhealthy half is eliminated and the remaining half is copied to create a population of original size. (iii) The elimination-dispersion step: with a certain probability, the bacteria are reset to a new position modeling the disturbances natural species of E. coli bacteria in the environment. Chemotaxis occurs in the innermost loop, reproduction in the central loop and dispersion-elimination in the outermost loop.

3.3.2 PTS technique for the reduction of the PAPR of the FBMC-OQAM signal

The scientific seine is full of researchers [49-51] dealing with PTS technology in the FBMC-OQAM system. The majority asserts that the application of PTS technology in the FBMC-OQAM system is different from OFDM, due to the overlap of FBMC-OQAM

symbols among them. Figure 3.5 shows that in this system, the length of each symbol is, the current symbol overlaps with the previous four symbols, which severely affects the value of the PAPR, taking into account the overlapping part of the previous symbols to determine the optimal phase vector of the current symbol. Consider X_m the block representing the input symbols for FBMC-OQAM where$X_m = (X_{m,0}X_{m,1} \dots X_{m,N\text{-}1})^T$, $0 \leq m \leq$M-1. According to the PTS technology, this block is divided into V sub-blocks, as mentioned earlier in the OFDM system, where $X_m = \sum_{v=0}^{V-1} X_m^v$ such as $X_m^0, X_m^1, \dots, X_m^{V-1}$, these sub-blocks are then multiplied by the phase factor, to which reference has been made previously. The "OQAM offset 1`mapping of sub-blocks$\{X_m^0 X_m^1 X_m^{V-1}\}_{m=0}^{M\text{-}1}$features the actual symbol $\{a_{m'}^1 a_{m'}^2 \dots a_{m'}^{V-1}\}_{m'=0}^{2.M\text{-}1}$, d'according to equation (1.32). Before proceeding to the determination of the optimal phase vector for each block, we must introduce the function g$\{X_m\}$, which represents the symbol of a sub-block of rank m , in accordance with the following relation :

$$\text{g}\{X_m\}(\text{n}) = \sum_{m'=2.m}^{2.m+1} \sum_{k=0}^{N\text{-}1} a_{m',k}.\text{h}(\text{n-m}'\frac{NL}{2}) e^{j\frac{2\pi k}{LN}n} e^{j\varphi}\text{m}', \text{k}, \tag{3.8}$$

Where; $\text{m}\frac{NL}{2} \leq n \leq m\frac{NL}{2} + 4.5NL - 1$

The temporal sequence of FBMC-OQAM, which extends from the first symbol to the m symbol, can be expressed in the following relation:

$$S_m(\text{n}) = \sum_{q=0}^{m} g\{X_q\}\ (\text{n}), \tag{3.9}$$

When applying the C-PTS technique to the time signal $S_m(n)$ represented by equation (3.17), where the symbols were considered to extend from the first symbol to the $m^{eme} - 1$ symbol, the PAPR would have already been reduced previously. With regard to the symbol m, the PAPR is reduced as follows:

$$\hat{\text{S}}_m(n) = \sum_{q=0}^{m\text{-}1} \hat{\text{g}}\{X_q\} + \sum_{i=0}^{V\text{-}1} g\{X_m^i\} cos\left(\frac{2\pi\hat{v}_{i,m}}{w}\right) + \sum_{i=0}^{V\text{-}1} g\{jX_m^i\} sin\left(\frac{2\pi\hat{v}_{i,m}}{w}\right), \tag{3.10}$$

While:

$$\hat{\text{g}}\{X_q\} = \sum_{i=0}^{v\text{-}1} g\{X_q^i\} \cos\left(\frac{2\pi\hat{v}_{i,q}}{w}\right) + \sum_{i=0}^{V\text{-}1} g\{jX_q^i\} sin\left(\frac{2\pi\hat{v}_{i,m}}{w}\right), \tag{3.11}$$

The PAPR can be calculated for the time signal in the n∈ υ_m domain according to the following relation:

$$PAPR_m=\frac{\max_{n\in\psi_m}|\hat{s}_m(n)|^2}{\frac{1}{4.5NL}\sum n\in\psi_m|\hat{s}_m(n)|^2}, \tag{3.12}$$

Where; $\psi_m=\left[m\frac{NL}{2}, m\frac{NL}{2}+4.5NL-1\right]$

The optimal phase vector can be determined for the lowest possible value of the $PAPR_m$ as follows:

$$(\hat{v}_{0,m}, \hat{v}_{1,m}, \hat{v}_{V-1,m})= =\underset{v_{i,m}\in\{0,1,\ldots,W-1\}}{argmin(PAPR_m)}, \tag{3.13}$$

The PTS requires lateral information (SI), represented by an optimal phase vector to restore the original signal at the level of the FBMC-OQAM receiver, where the length of SI is equal to M.(V-1) $log_2(w)$bits.

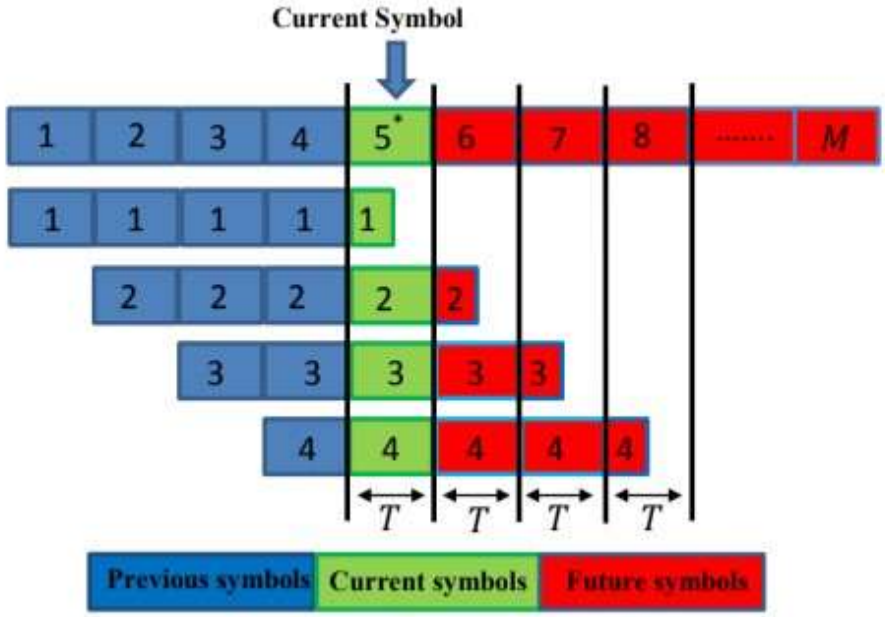

Figure 3.3-Overlapping symbols in the FBMC-OQAM system.

When the PTS technique is applied in the FBMC-OQAM system, the computational complexity can be estimated by determining the number of multiplications (RM_S) and real additions (RA_S) involved in this design. For the function g, the number of multiplications

$RM_{S_g} = NL.log_2(NL) + 2N(4L+1)$, , while the number of additions is $RA_{S_g} = 2Nl.log_2$, the number of multiplications and additions making it possible to calculate the PAPR during each domain ψ_m are;$RM_{S_{PAPR_m}} = 4NL, RA_{S_{PAPR_m}} = 4NL - 1$, respectively.

The determination of the computational complexity of the PTS technique includes the determination of the complexities of the optimal phase vector, that of calculating the g function as well as that of calculating the$PAPR_m$. Finally, the computational complexities of the PTS technique can be summarized by the following:

For W=2, permanently the term, sin $(\frac{2\pi\hat{v}_{i,q}}{w})$ = 0 :

$$RM_S = 16\ \text{MVNL}\ (2^V + N) + (4\text{NL}+1)\text{MN},$$
$$RA_S = 8\text{MNL}\ (2\text{NV-V}+2\text{V}\times 2^V - 2^V), \qquad (3.14)$$

For W≠ 2, not always the term, $\sin\left(\frac{2\pi\hat{v}_{i,q}}{W}\right) = 0$:

$$RM_S = 2\text{MV}\left(NL.log_2(NL) + 2N(4L+1)\right) + 9MVLNW^{V-1},$$
$$RA_S = 2\text{MV}.(2NL.log_2(NL) + 7NL) + \left((9V - O.5)LN - 1\right)MW^{V-1}, \qquad (3.15)$$

Thus, this research work will address the problems encountered by the PTS technology in the FBCM-OQAM system such as:

- Solving the computational complexity problem that concerns the number of multiplications and additions used in the search for the optimal phase vector ;
- Reduce the length of the IF that is likely to cause a decrease in the flow rate ;
- The difficulty of restoring the SI at the level of the receiver ;
- Solve the problem of the overlapping structure of the FBMC-OQAM system.

Several researchers have worked on the problem of the overlapping structure which can reduce the computational complexity of the FBMC-OQAM system, among them; the author in [50] proposed the so-called S-PTS (Sparse Partial Transmit Sequence) scheme, in this scheme; the first step consists in dividing the interdependent transmission data into several sub-blocks, then detecting and recording the location of the random maximum peak of the time domain FBMC- OQAM signals derived from the superposition of the subblocks. The second step returns the recorded location to the sub-blocks and uses phase factors to optimize the phase of each data item on the corresponding position of the sub-blocks. This makes it

possible to reduce the superposition of the data on this location point but does not modify any data on other positions, so as to reduce the PAPR of the FBMC-OQAM signal, the algorithm of the S-PTS scheme can be found in [50]. The difference between the C-PTS and S-PTS schemes lies in the fact that all data are taken into account to select the optimal combination of phase rotation in the C-PTS scheme, while the proposed S-PTS scheme only executes the data phase optimization operation with a high peak, without modifying the data on the other positions. This means that the computational complexity of the proposed S-PTS scheme would be good lower than that of the C-PTS scheme. Moreover, as the probability of occurrence of the maximum peak of the FBMC-OQAM signals is relatively low, only a few maximum peaks should be processed with phase optimization so that its impact on the average power of the signals FBMC-OQAM be imperceptible. It is explained theoretically that the proposed S-PTS scheme can lead to a significant decrease in the PAPR of FBMC-OQAM signals. The author in [51] proposed a new optimization structure for the PTS technique, called P-PTS (Pretreated Partial Transmit Sequence), in order to reduce the FBMC-OQAM signal PAPR. In due to the overlapping structure of the FBMC-OQAM signals, it takes into account several blocks of data when reducing the peak power, instead of each block of data independently. This technique has two steps; the first uses a scheme optimization common to several overlapping symbols, in which the sequences of phase rotation of the current symbol are determined and optimized according to the symbols overlapping precedents, the second uses a new segment scheme based on the PTS technique, similar to the C-PTS. The main idea is to split the FBMC-OQAM signals overlapping into a number of segments, then divide and multiply some sub-blocks separated by different phase rotation factors in each segment. The comparison of the two schemes leads to the following conclusions; P-PTS makes it possible to obtain from much better PAPR reduction performance with less computational complexity. in addition, the P-PTS introduces two key parameters V and U, which makes it possible to use different combinations of parameters and facilitate the negotiation of complexity and performance of calculation. Compared to the S-PTS scheme, different combinations of parameters can be easily exchanged between the computational complexity and the PAPR reduction performance.

3.4. New PTS technique for the reduction of the PAPR of the OFDM signal

In this section, we will discuss the treatment of several problems encountered by PTS technology and among them [52]:

- To solve the problem of IFFT sub-blocks, where V, which corresponds to the number of IFFT blocks included in the design of the conventional PTS technique, is a primary parameter for reducing the value of the PAPR. Therefore, increasing the number V means an increase in the number of IFFT blocks, which complicates the design of the PTS. Thus, this section tends to suggest a new model in order to overcome the problems of PTS; this technique is called "New-PTS".
- But the second problem is the number of research processes in determining the minimum value of the PAPR, despite the existence of several techniques to address this issue, mentioned earlier. In this chapter, we suggest a new technique to limit the number of research processes, this technique, developed by us which we have called "CR-New-PTS".

3.4.1 New-PTS

In this technique, the input data block X of length N is partitioned into V disjoint sub-blocks of length N, denoted $X^0, X^1, \dots, X^{V-1}$, such as X=$\sum_{v=0}^{V-1} X^v$, where X=$[X_0, X_1, \dots, X_{N-1}]$ represents the complex symbols in the frequency domain of the OFDM signal and X$\left(X^i\right) \cap X\left(X^j\right) = \{\emptyset\}$for i≠ j , where $\{\emptyset\}$ is the empty set and X$(U) = \{i|u_i \neq 0\}$ is the support of a vector U $= [u_0, u_1, \dots, u_{N-1}]$ In this technique, each X^i is chosen to have a uniform weight equal to N/V . There are generally three possible partitioning schemes on the OFDM block, including adjacent, interlaced and random partitions. The objective of the new PTS technique (New-PTS) is to eliminate IFFT blocks by choosing partitions interleaved which are given by:

$$X^v = [X_0^v, X_1^v, \dots, X_{N-1}^v]/X_i^v \begin{cases} X_i, & i \in \Omega_v \\ 0, & i \in \Omega_v^c \end{cases}, \tag{3.16}$$

Where $\Omega_v = \left\{v + m.V | m \epsilon \{0,1, \dots, N/V - 1\}\right\}$,$v = 0,1, \dots, V-1$ and Ω_v^c is the set of the complement of Ω_v in $\Lambda_N = \{0,1, \dots, N-1\}$.

The signal subsequence$x^v = [x_o^v, x_1^v, x_{N.L-1}^v]$, is generated by applying the "IFFT operation of $N.L$ point for each sub-block of symbolX^v, taking into account the insertion of $N.(L-1)$ zeros in the middle of eachX^v. The signal subsequence $x^v(n)$ is given by the following relation (the demonstration of this relation can be found in Appendix C"):

$$x^{v}(n) = \frac{1}{V}\sum_{i=0}^{V-1} x\left(n - i\frac{N.L}{V}\right) e^{j\left(\frac{2\pi}{v}\right)iv}, \tag{3.17}$$

Where $\mathrm{x}\left(n - i\frac{N.L}{V}\right)$ indicates the cyclically shifted version (VDC) to the left of the discrete-time OFDM symbol $\mathrm{x}(n)$ by the integer $\frac{N.L}{V}$, the x^{v} sub-sequences are added together after multiplication by a rotation factor$b_v = e^{j\frac{2\pi}{W}\gamma_v}$, such as:

$$x'(n) = \frac{1}{V}\sum_{v=0}^{V-1} b_v x^{v}(n), \tag{3.18}$$

Replacing the expression $x^{v}(n)$ in equation (3.18) we obtain the following:

$$x'(n) = \sum_{i=0}^{V-1}\left(\frac{1}{V}\sum_{v=0}^{V-1} b_v e^{j\left(\frac{2\pi}{V}\right)iv)} x\left(n - i\frac{N.L}{V}\right)\right), \tag{3.19}$$

With $B_i = IFFT\{b_o, b_1, b_{V-1}\} = \frac{1}{V}\sum_{v=0}^{V-1} b_v e^{j\left(\frac{2\pi}{V}\right)iv}$, $x'(n)$ becomes as follows:

$$x(n) = x_B(n) = \sum_{i=0}^{V-1} B_i\, x\left(n - i\frac{N.L}{V}\right), \tag{3.20}$$

Knowing that $\mathrm{b_v} \in \left\{e^{\mathrm{j}\frac{2\pi}{\mathrm{w}}\gamma_{\mathrm{v}}} | \gamma_{\mathrm{v}} \in \{0,1,\dots,\mathrm{w}-1\}\right\}$, so there are w^{v-1} possibilities for the phase vector $\mathrm{b}= [b_0, b_1, \dots, b_{V-1}]$ with $b_0 = 1$, based on this, all possible candidates can be saved so that $\mathrm{B}= [B_0, B_1, \dots, B_{V-1}]$. The backup of B in the random access memory (RAM) will be in the form of a matrix whose size is $\mathrm{V}\times W^{V-1}$, in addition, each candidate has an appropriate (ad) address which represents an integer between 0 and $W^{V-1} - 1$, and which can be written as follows :

$$\mathrm{Ad}= 0.W^{V-1} + \gamma_1 W^{V-2} + \cdots + \gamma_{V-1} = \langle o, \gamma_1, \dots, \gamma_{V-1}\rangle W, \tag{3.21}$$

Where $\langle . \rangle$ W is the writing of the integer (ad)in the basic numbering system$W$. All the possible candidates of the vector B are stored in the RAM memory as a function of the appropriate address(ad), such that:

$$\mathrm{RAM}(ad) = B = IFFT\left\{1, e^{j\frac{2\pi}{w}\gamma_1}, \dots, e^{j\frac{2\pi}{w}\gamma_{V-1}}\right\}, \tag{3.22}$$

In order to choose the signal to be transmitted $x_{\hat{B}}(n)$ with the minimum PAPR corresponding to the "$\widehat{Ad}$ address which is obtained by:

$$\widehat{Ad} = \begin{cases} \underset{0 \le Ad \le W^{V-1}-1}{argmin} \left(\underset{0 \le n \le N.L-1}{max|x_B(n)|} \right), \\ B = RAM(Ad) \end{cases} \quad (3.23)$$

Where, $argmin$ locates the minimum element of the value $max_{0 \le n \le N.L-1}|x'(n)|$, and returns the corresponding index of this element in the variable(Ad) . The optimal rotation vector $\hat{b}$ can be:

$$\hat{b} = \left[1, e^{j\frac{2\pi}{w}\hat{\gamma}_1}, \dots, e^{j\frac{2\pi}{w}\hat{\gamma}_{v-1}}\right], \quad (3.24)$$

Where$\langle 0, \hat{\gamma}_1, \dots, \hat{\gamma}_{V-1} \rangle_w = \widehat{Ad}$, after using equation (3.21), where the transmission signal $x_{\hat{b}}(n)$ is given by the following relation:

$$x_{\hat{B}}(n) = \sum_{i=0}^{V-1} \hat{B}_i x\left(n - i\frac{N.L}{V}\right), \quad (3.25)$$

Where:

$$\hat{B} = \left[\hat{B}_0, \hat{B}_1, \dots, \hat{B}_{V-1}\right] = RAM\left(\widehat{Ad}\right), \quad (3.26)$$

Figure 4.1 shows the OFDM transmitter using the New-PTS scheme. It is well known that the PAPR reduction performance of the PTS depends on the partitioning scheme of the IFFT sub-blocks; in contrast, these same IFFT sub-blocks are eliminated in the New-PTS.

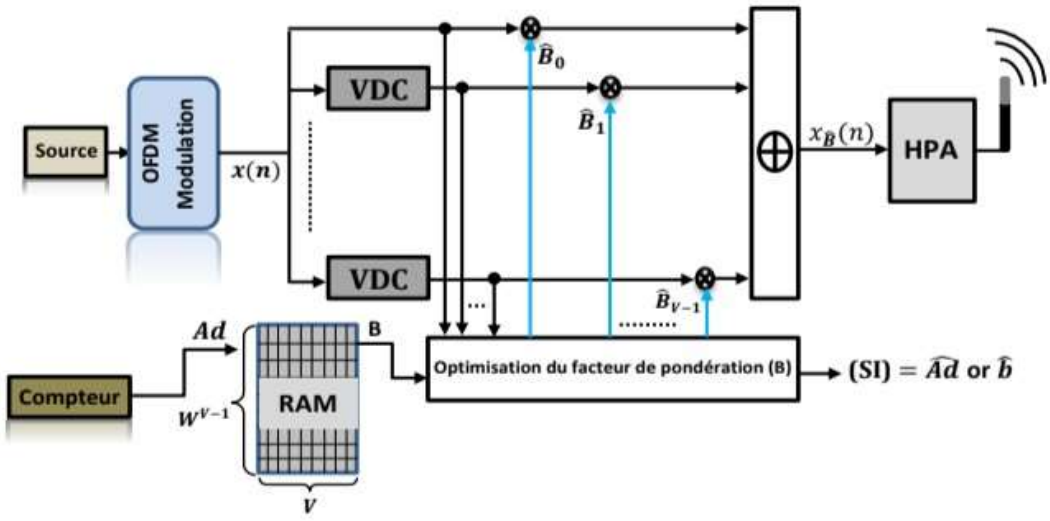

Figure 3.4-Functional diagram of the new PTS (New-PTS).

A transmitter is necessary to send the SI ($\widehat{Ad}$ or $\hat{b}$) in order to correctly restore the initial input symbol sequence at the receiver, which causes a certain loss of data transmission rate. Therefore, many researchers are "interested in the transmission of SI without degradation of system performance [53-54].

3.4.2 Complexity reduction technique

The complexity reduction technique (CR-New-PTS) focuses mainly on solving the problem of the number of search processes to obtain the optimal vector, which corresponds to the lowest PAPR. Indeed, the New-PTS technique proposed in this chapter does not take into account the reduction in the number of search processes which is equal to W^{V-1} to obtain the optimal address. By considering V sub-blocks, we then form V_b groups; containing V_a sub-blocks, that is to say that V= $V_b \times V_a$, the V_b sub-blocks are added up and multiplied by the phase factor b_u where $u \in \{o, 1, \dots V_a - 1\}$ with $b_0 = 1$. The selection of the groups is carried out using an index (index) obtained by the random change of the positions of the elements of the vector$\pi = [0\ 1 \dots V - 1]$. The step of constitution of the subgroups X'_u from the sub-blocks $X^0, X^1, \dots, X^{V-1}$ is represented by the following equation:

$$X'_u = \left[X^{index(V_b.u+0)} \dots \dots X^{index(V_b.u+V_b-1)}\right], \tag{3.27}$$

Where:$u \in \{o, 1, \dots V_a - 1\}$ and index(i) designates the elements of a vector caused by the random interleaver of the vectorπ; then the IFFT operation is applied according to the following relation, to obtain the time signal:

$$x'(n) = IFFT\left\{\sum_{u=0}^{V_a-1} b_u \sum_{m=0}^{V_b-1} X^{index(V_b.u+m)}\right\}, \tag{3.28}$$

Using the linearity of the IFFT operation leads to the following:

$$x'(n) = \sum_{u=0}^{V_a-1} b_u \sum_{m=0}^{V_b-1} x^{index(V_b.u+m)}(n), \tag{3.29}$$

Where: $x^{index(V_b.u+m)}(n) = IFFT\left\{X^{index(V_b.u+m)}\right\}$,

Applying the mathematical rules of New-PTS previously used to eliminate the IFFT blocks, the expression (3.29) becomes:

$$x'(n) = x_B(n) = \sum_{i=0}^{V-1} B_i\, x\left(n - i\frac{N.L}{V}\right), \tag{3.30}$$

Where:

$$B_i = \frac{1}{V}\sum_{u=0}^{V_a-1} b_u \sum_{m=0}^{V_{b-1}} e^{j\left(\frac{2\pi i}{V}\right).index(V_b.u+m)}, \tag{3.31}$$

The addresses used to read the B_i data stored in the RAM can be calculated. This is achieved by making a counter, which counts from count=0 to short= $W^{V_a-1}-1$; the decimal value, namely the count, is converted into a flower in the system of the base number W so that $(count)_{10} = \langle o, \gamma_1, \dots, \gamma_{V_a-1}\rangle_w$ at each increment, such that:

$$Ad = \sum_{u=1}^{V_a-1} \gamma_u \sum_{m=0}^{V_b-1} W^{index(V_b.u+m)}, \tag{3.32}$$

The address(Ad) that corresponds to the optimal vector $\hat{B} = \left[\hat{B}_0, \hat{B}_1, .., \hat{B}_{V-1}\right]$ to obtain the transmission signal $x_{\hat{B}}(n)$ with the minimum PAPR is obtained as follows:

$$\widehat{Ad} = \underset{B=RAM(Ad)}{argmin}\left(\underset{0 \le n \le N.L-1}{max|x'_B(n)|}\right), \tag{3.33}$$

The transmission signal is given by:

$$x_{\widehat{B}}(n) = \sum_{i=0}^{V-1} \widehat{B}_i x\left(n - i\frac{N.L}{V}\right), \tag{3.34}$$

This technique is repeated N_{iter} iterations; where: $x(n)$and $x_{\hat{B}}(n)$ are replaced by$x_j(n)\ and\ x_{j+1}(n)$, respectively; then the optimal address (Ad) can be calculated for each iteration. Thus, to achieve this goal, let's define the operation $\underset{w}{\oplus}$ between the two integers A and B between 0 and $W^{V-1}$to calculate c, where:

$$c = A \underset{w}{\oplus} B, \tag{3.35}$$

We follow these steps:

A and B are converted from the decimal system to the basic numerical system W, where:

$$\begin{aligned} A &= \langle 0, a_1, \dots, a_{V-1}\rangle_w, \\ B &= \langle 0, b_1, \dots, b_{V-1}\rangle_w, \end{aligned} \tag{3.36}$$

$c_1, \dots, c_{V-1}$ Are calculated where:

$$c_i = (a_i + b_i) mod\ W \quad , \quad i = 1, \dots, V-1, \tag{3.37}$$

Calculate C', where$\langle o, c_1, \dots, c_{V-1} \rangle_w$ is converted to a decimal value, such as:

$$C' = 0.W^{V-1} + c_1 W^{V-2} + \cdots + c_{V-1}, \tag{3.38}$$

Finally:

$$C = A \oplus_{|w} B = C', \tag{3.39}$$

The optimal address for each iteration can be found through this process as follows:

$$Ad_{j+1} = Ad_j \overset{\oplus}{_w} \widehat{Ad}_{j+1}, \tag{3.40}$$

Where:$\widehat{Ad}_{j+1}$ est l'adresse optimale pour obtenir le PAPR minimal du signal temporel$x_j(n)$, l'adresse initiale est considérée comme égale à zéro$(Ad_0 = 0)\ and\ x_0(n) = x(n)$. The number of search processes for CR-New PTS is then$N_{iter} W^{V_a - 1}$.

3.5 Analysis of the computational complexity for the New-PTS and C-PTS techniques

It is agreed that N.L IFFT points require $(N.L/2)\log 2\,(N.L)$ complex multiplications and $(N.L)\log 2\,(N.L)$ complex additions. The C-PTS scheme consists of V IFFT sub-blocks. Therefore, the number of complex multiplications $(n_{mul})$and the number of complex additions $(n_{add})$to perform V IFFT operations are respectively $(V.N.L/2)\log 2\,(N.L)$ and$(V.N.L)\log 2\,(N.L)$. In addition,$W^{V-1}.(V-1).N.L$ complex multiplications and additions are necessary to combine the signals of V sub-blocks to obtain the candidate W^{V-1}in order to search for the minimum PAPR. Thus, the total number of multiplications $\left(n_{c-pts,mul}\right)$ and that of additions $\left(n_{c-pts,add}\right)$for the C-PTS scheme are given by the following relations:

$$\begin{aligned} n_{c-pts,mul} &= (V.N.L/2)\log 2\,(N.L) + (V-1).N.L.W^{V-1}, \\ n_{c-pts,add} &= (V.N.L)\log 2\,(N.L) + (V-1).N.L.W^{V-1}, \end{aligned} \tag{3.41}$$

As for the proposed PTS system (New-PTS), it requires only one IFFT block. Therefore, the number of complex multiplications (n_{mul}) and that of complex additions (n_{add}) to perform an IFFT operation are $(N.L/2)\log 2(N.L)$ and $(N.L)\log 2(N.L)$, respectively. There are W^{V-1} possible candidates to have the minimum of the PAPR of the transmitted signal, where

the total number of multiplications $(n_{New-pts,mul})$ and that of the additions $(n_{New-pts,add})$ for the New-PTS scheme are given by the following relations:

$$n_{New-pts,mul} = (N.L/2)\log 2\,(N.L) + (V-1).N.L.W^{V-1},$$
$$n_{New-pts,add} = (N.L)\log 2\,(N.L) + (V-1).N.L.W^{V-1}, \quad (3.42)$$

As a complex multiplication is equivalent to four complex additions [54], the complexity can be expressed in the following way:

$$C_{c-pts} = n_{c-pts,mul} + \frac{n_{c-pts,add}}{4},$$
$$C_{New-pts} = n_{New-pts,mul} + \frac{n_{New-pts,add}}{4}, \quad (3.43)$$

The Computational Complexity Reduction Ratio (CCR) is an important parameter in the analysis of the computational complexity for the conventional technique (C-PTS) compared to a recent technique (New-PTS). The CCRR can be calculated using the following equation:

$$CCRR_{New-pts/c-pts} = \left(1 - \frac{C_{New-pts}}{C_{c-pts}}\right) \times 100\%, \quad (3.44)$$

If the value of the $CCRR_{New-pts/c-pts}$ is negative, this means that the C-PTS is better than the New-PTS in terms of computational complexity. If the values are equal to zero, then they have the same computational complexity. While in the case where the values are positive, the recent technique is better, analyzing the results of Table 3.1, we notice the following:

Table 3.1-CCRR of the New-PTS compared to the C-PTS.

	N		
(V,W)	64	256	1024
(16,2)	0.0146 %	0.0183 %	0.0220 %
(8,4)	0.0293 %	0.0366 %	0.0439 %
(8,2)	3.5959 %	4.4492 %	5.2852%
(4,4)	6.8182 %	8.3333 %	9.7826%
(4,2)	33.3333 %	37.5000 %	40.9091 %

The CCRR values are positive values regardless of the parameters $V, W and\ N$ which shows that New-PTS is better than C-PTS. This is due to the elimination of IFFT sub blocks.

The values of the CCRR vary according to the evolution of the parameters $N, W\ and\ N$, for example, when fixing(V, W) and from the increase in the value of N the CCRR increases, while in the case$V = 4$, the values of the CCRR increase rapidly by varying $W = 4$ to $W = 2$ for whatever the values of$N$.

3.6 Conclusion

In this case, the PTS technology is sufficiently clear to replace the OFDM and FBMC-OQAM PAPR systems. Unfortunately, the PTS technology is confronted with a problem of computational complexity in multiple IFFT blocks and numerous search processes. Making it possible to obtain the optimal phase factor. Without asking other questions, there are always many innovative solutions. To do this, a new PTS technique is proposed, which aims to eliminate IFFT blocks. Therefore, a reduction in computational complexity in a number of complex multiplications and additions is confirmed, thereby confirming the significant results of the analysis of CCRR parameters. In addition, the CR-New-PTS technology is recommended for use in search engines of this type. This month, this chapter presents a proposed method that replaces the main one on the MED decoder for the SI restoration of the system at the reception site without reserving additional bits for reference. the main information. The results of the simulation make it possible to compare the proposed techniques: CR-New-PTS, New-PTS and N-PTS, as well as the conventional PTS method between the terms BER and CCDF. The results, in essence, show that the proposed method is more efficient in the complex calculation, as well as more efficient in the reduction of the PAPR and the amplification of the BER.

Chapter Ⅳ

Simulation results

4.1 Introduction

This chapter focuses on analyzing the performance of the proposed technique through a series of numerical simulations aimed at evaluating its effectiveness in reducing the Peak-to-Average Power Ratio (PAPR) in OFDM systems. The simulations are carried out in a suitable environment that enables comparison between the proposed New-PTS method and conventional PTS-based techniques in terms of both performance and computational complexity. The simulation process includes the investigation of key system parameters such as the number of subcarriers and the number of phase rotation factors, in addition to analyzing the Bit Error Rate (BER) performance under an AWGN channel. The results are presented using CCDF curves to highlight the effectiveness of the proposed method in reducing PAPR compared to existing approaches, while also emphasizing the trade-off achieved between performance and complexity.

4.2 Objectives of the simulation

This simulation aims to address one of the main technical challenges in multicarrier communication systems (OFDM), namely the high Peak-to-Average Power Ratio (PAPR), through the following objectives:

a. Propose an enhanced technique to reduce computational complexity; the primary goal is to develop a new version of the PTS technique, referred to as New-PTS, which significantly reduces the number of computational operations particularly IFFT computations without negatively affecting system efficiency.
b. Achieve a balance between performance and complexity; the study aims to achieve a noticeable reduction in PAPR while maintaining a low computational cost, thereby enhancing overall system performance without excessive resource consumption.
c. Improve transmission quality in wireless systems; by reducing PAPR, the proposed technique helps minimize signal distortion caused by power amplifiers operating in non-linear regions, resulting in improved transmission quality and communication reliability.
d. Evaluate the proposed technique through numerical simulations; the study relies on a series of digital simulations to compare the performance of the proposed technique with traditional methods (such as O-PTS, I-PTS, GD-PTS, and ABC-PTS), in terms of PAPR, Bit Error Rate (BER), and computational complexity.

4.3 Simulation Results and Discussion

In this section, we first compare the CR-New-PTS method with the I-PTS, GD-PTS, ABC-PTS, BFO-PTS, Random Search PTS (RS-PTS), and Optimum PTS (O-PTS) methods in terms of PAPR reduction performance and the number of search processes in the OFDM system. Secondly, the BER performances of the CR-New-PTS and O-PTS techniques are shown both with and without the use of the High Power Amplifier (HPA). Comparisons are carried out using both 16-Quadrature Amplitude Modulation (16-QAM) and Quadrature Phase Shift Keying (QPSK). The simulation parameters used in this study are provided in Table 4.1, where the convolutional coding rate (CC for Convolution Coded) is ½, the constraint length is 7, the first register is $(g1 = 133)$, and the second register is $(g2 = 171)$. The possible combinations of phase factors are $\{1, -1\}$ and $\{1, -1, j, -j\}$ for $W = 2$ and $W = 4$, respectively. The authors aim, on the one hand, to meet the data transmission requirements of future wireless systems and, on the other hand, to suggest an extension of the results reported in this work; consequently, all results are reported at CCDF = $10^{-5}$and BER = 10^{-7}.

Table 4.1: Simulation Parameters.

Parameters	Quantity	Value
16-QAM, QPSK	Type of modulation	4, 2 bits
N	Number of subcarriers	256
V	Number of sub-blocks	16, 8, 4
W	Number of phase factors	2, 4
SSPA	Amplifier	-
$IBO\ (dB)$	Input Back-off	0, 3, 6
p	Smoothness factor	0.5
L	Oversampling factor	4

4.3.1 Performance of Methods for PAPR Reduction

Figures 4.1 and 4.2 show the CCDF curves of the PAPR for the previously compared schemes for 16-QAM and QPSK, respectively. The CCDF curves of the original OFDM PAPR are also included for comparison purposes. As shown in Figure 4.1, the PAPR of the original OFDM signal is 12 dB Let us recall that the number of search processes in the O-PTS method is W^{V-1}. Taking $W = 2$ and $V = 16$. In O-PTS, where exhaustive search is used, a PAPR

value of is obtained 12 dB. Let us recall that the number of search processes in the O-PTS method is W^{V-1}. By taking into account $W = 2$ and $V = 16$. In O-PTS, where exhaustive search is used, a PAPR value of 6.8 dB is obtained, with $W^{V-1} = 2^{15} = 32768$ searches: by taking $W = 2$ and $V = 8$, a PAPR value of 7.91 dB is obtained with $W^{V-1} = 4^3 = 64$ searches. Moreover, when $W = 4$ and $V = 4$, the PAPR value is 9.56 dB with $W^{V-1} = 4^3 = 64$ searches. In the case of the I-PTS technique, where the number of search processes is $W.(V-1) = 2.(16-1) = 30$ searches. The GD-PTS technique, on the other hand, the number of search processes is proportional to $C_r^{V-1}.W^r.I$. where I is the maximum number of iterations, $C_r^{V-1} = \frac{(V-1)!}{r!(V-1-r)!}$ is the binomial coefficient, and r is the Hamming distance; this technique yields a PAPR value of 8 dB with a number of search processes equal to $C_2^{15}.2^2.3 = 1260$, RS-PTS is used with $SN = 1024$ as the number of search processes, which corresponds to the number of phase vectors that are randomly selected using two states: −1 or +1. The resulting PAPR value is 7.5 dB. In the ABC-PTS technique, where the number of food sources (FN) and the maximum number of cycles (MC) are used as input parameters, the number of search processes is given by ; $I = FN \times MC$.

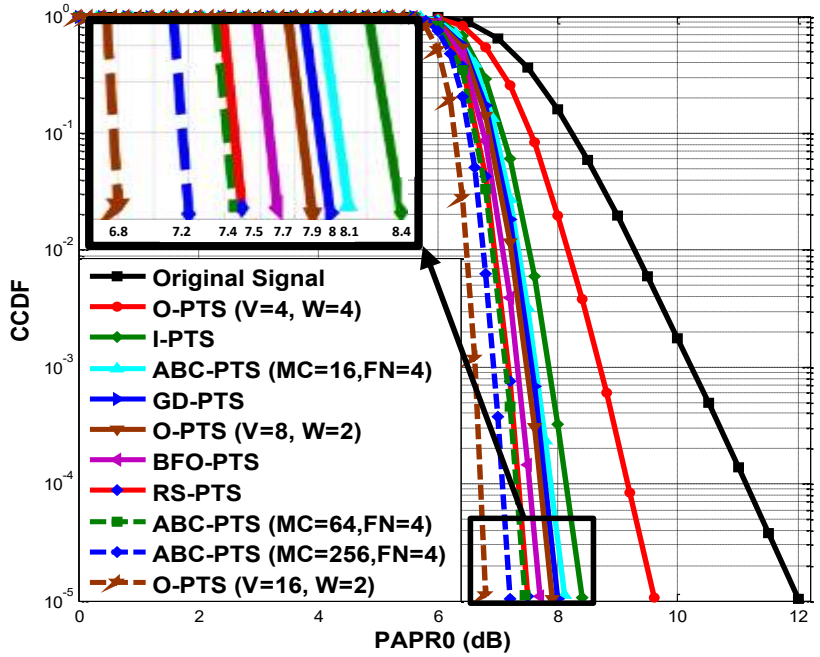

Figure 4.1: Comparison of PAPR reduction performance of the O-PTS, ABC-PTS, RS-PTS, BFO-PTS, GD-PTS, and I-PTS techniques, as well as the original OFDM signal, for 16-QAM.

For the following values of I, $I = 4 \times 16 = 64, I = 4 \times 64 = 256$ and $I = 4 \times 256 = 1024$, the corresponding PAPR values are 8.1 dB, 7.45 dB, and 7.19 dB, respectively. As for the RS-PTS technique, with $SN = 1024$, it exhibits performance similar to that of ABC-PTS with only 256 search processes. In BFO-PTS, the input parameters are as follows: S = 6, Nc = 4, Ns = 2, Nre = 4, Ned = 2, Ped = 0.25, Msw = 10, Wr = 10, and Wa = 0.2, where S is the size of the bacterial population, Nc is the number of chemotactic steps, Ns is the number of swimming steps, Nre is the number of reproduction steps, Ned is the number of elimination-dispersal steps, Ped is the elimination-dispersal probability, Msw is the magnitude of the swarming effect, Wa is the coefficient of the attractive effect, and Wr refers to the coefficient of the repulsive effect. The number of search processes is then $S \times N_c \times N_s \times N_{re} \times N_{ed} = 6 \times 4 \times 2 \times 4 \times 2 = 384$; consequently, the PAPR value is 7.7 dB. Figure 4.2 shows performance similar to that of Figure 4.1, with a difference of nearly 0.2 dB for all methods.

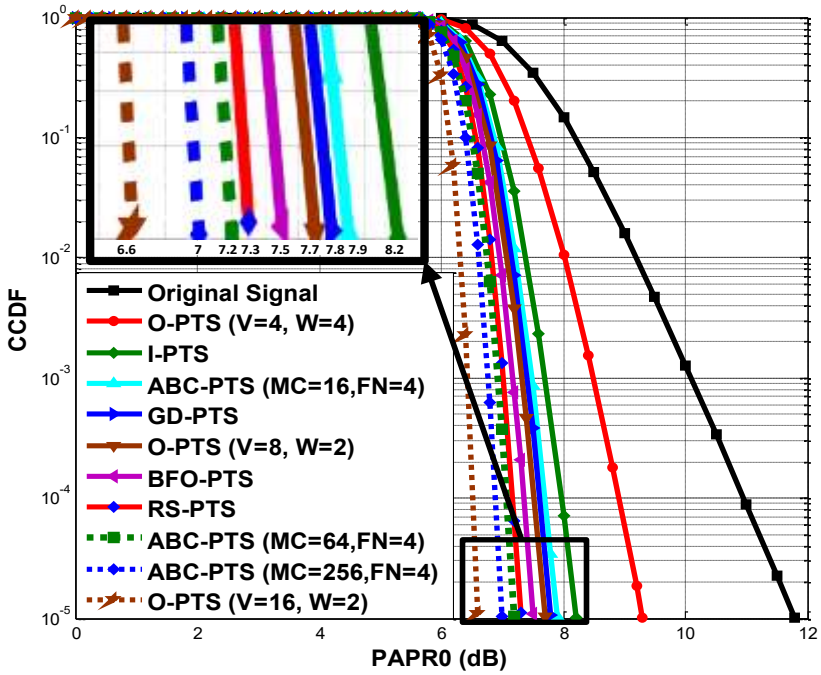

Figure 4.2: Comparison of PAPR reduction performance of the O-PTS, ABC-PTS, RS-PTS, BFO-PTS, GD-PTS, and I-PTS techniques, as well as the original OFDM signal, for QPSK.

Figures 4.3 and 4.4 show the PAPR reduction performance of the CR-New-PTS technique for 16-QAM and QPSK, taking into account various parameters affecting this technique, such as W, V and V_a at $\mathrm{CCDF} = 10^{-5}$. Moreover, the number of iterations used in this technique is

$N_{iter} = 2$ the PAPR value for $V = 16$, $W = 2$, and $V_a = 8$, the PAPR value is 7.17 dB and 7 dB for 16-QAM and QPSK, respectively, while the number of search processes is $2.2^7 = 256$, by setting $V = 8, W = 4$, and $V_a = 4$, the PAPR value is 8 dB and 7.82 dB for 16-QAM and QPSK, respectively, and the number of search processes is $2.4^3 = 128$. In the case where $V = 16, W = 2$, and $V_a = 4$, the PAPR value becomes 9.21 dB and 9.04 dB for 16-QAM and QPSK, respectively, while the number of search processes is $2.2^3 = 16$. Finally, for $V = 8, W = 4$, and $V_a = 2$, the PAPR value is 9.48 dB and 9.27 dB for 16-QAM and QPSK, respectively, and the corresponding number of search processes is $2.4^1 = 8$.

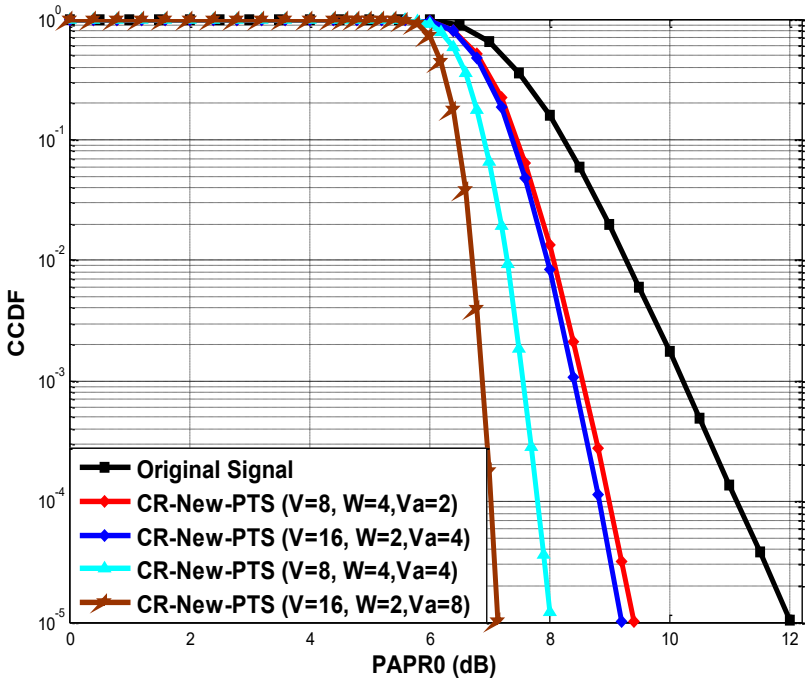

Figure 4.3: Comparison of PAPR reduction performance of the CR-New-PTS technique for different values of the parameters W, V, and V_a for 16-QAM.

In Figures 4.5 and 4.6, simultaneous comparisons are easily carried out between the proposed CR-New-PTS technique and other existing schemes. The objective is to highlight the strengths and weaknesses of each simulated technique for 16-QAM and QPSK modulations. It is demonstrated that the proposed new method is the most suitable for achieving the desired objectives in terms of PAPR reduction performance and the number of search processes. It is worth noting that the CR-New-PTS technique is very close to O-PTS in performance, compared to ABC-PTS. Consequently, at $\mathrm{CCDF} = 10^{-5}$, the PAPR value of the CR-New-PTS technique is 7.17 dB and 7 dB for 16-QAM and QPSK modulations, respectively, while

the number of search processes is 256. When using the same number of search processes in the ABC-PTS technique, the PAPR value becomes 7.45 dB for 16-QAM and 7.27 dB for QPSK, which represents a difference of 0.23 dB and 0.27 dB, respectively. The same PAPR values of 7.19 dB and 7 dB for 16-QAM and QPSK, respectively, can be obtained with the ABC-PTS technique using MC = 256 and FN = 4, and with the CR-New-PTS technique using $V_a = 8, V = 16$, and $W = 2$. In these cases, the number of search processes is 1024 and 256, respectively, leading to satisfactory improvements with a fourfold reduction in execution time.

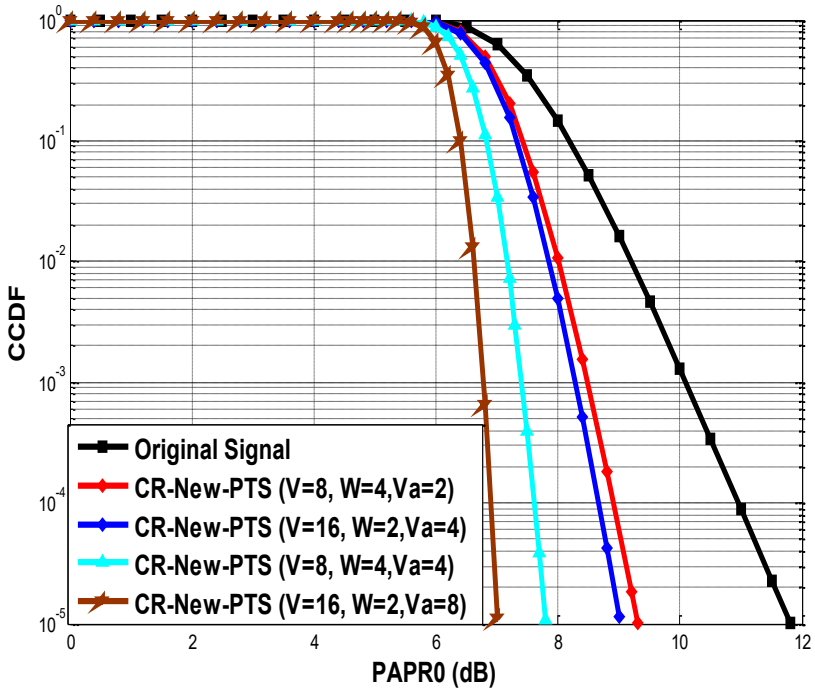

Figure 4.4: Comparison of PAPR reduction performance of the CR-New-PTS technique for different values of the parameters W, V, and V_a for QPSK.

Table 4.2 shows the search process complexity and the different PAPR values of the previously described PTS approaches, at CCDF $= 10^{-5}$, the PAPR value of the CR-New-PTS technique, for a search process count of 256, is only 0.4 dB higher than that of O-PTS, which requires 32,768 search processes. Consequently, CR-New-PTS exhibits a search complexity of only 256/32,768 = 0.78% compared to O-PTS.

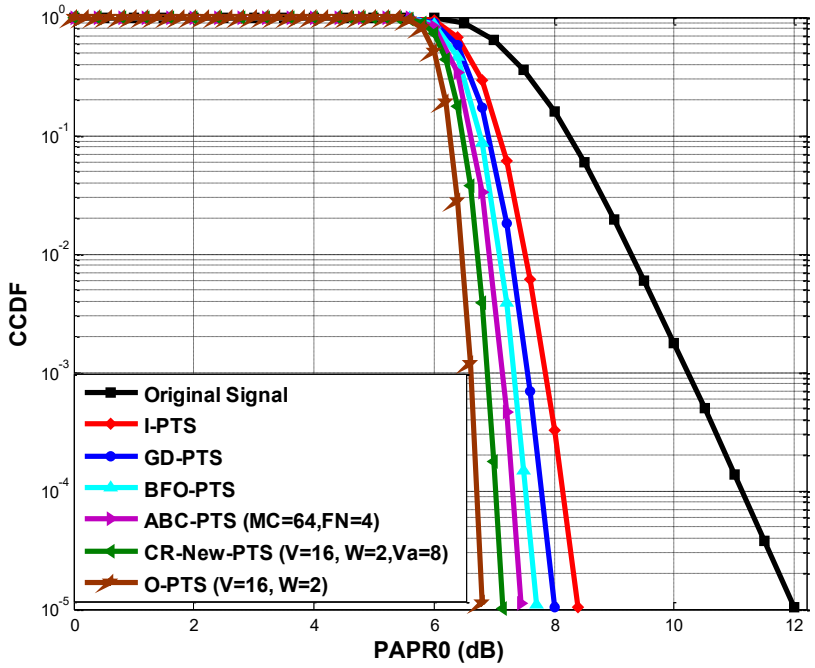

Figure 4.5: Comparison of PAPR reduction performance of the O-PTS, CR-New-PTS, ABC-PTS, BFO-PTS, GD-PTS, and I-PTS techniques, as well as the original OFDM signal, for 16-QAM.

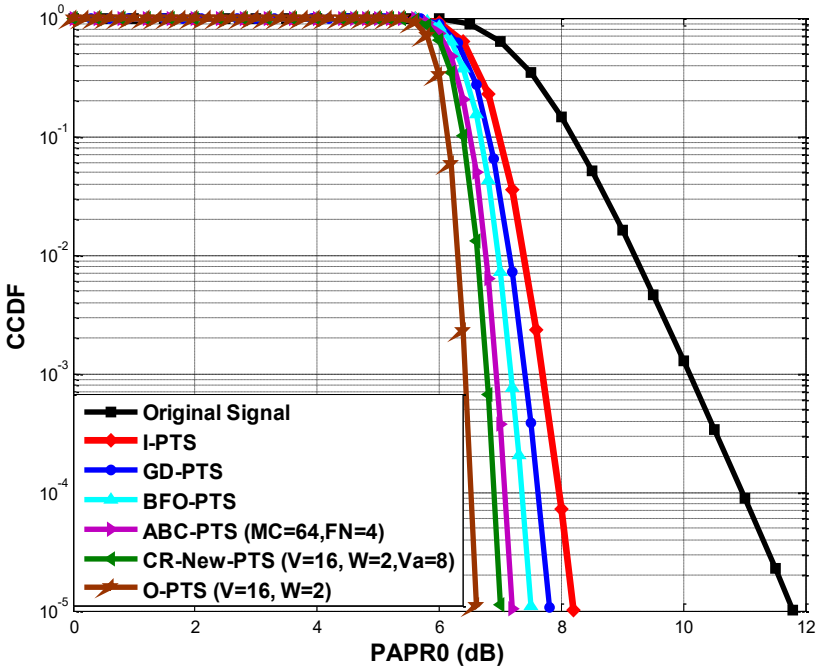

Figure 4.6: Comparison of PAPR reduction performance of the O-PTS, CR-New-PTS, ABC-PTS, BFO-PTS, GD-PTS, and I-PTS techniques, as well as the original OFDM signal, for QPSK.

Table 4.2: Complexity analysis of the different PTS techniques.

Méthode	Nombre de Processus de Recherches	PAPR (dB)	
		16-QAM	QPSK
Original	0	12	11.83
O-PTS ($V = 16, W = 2$)	32768	6.8	6.61
O-PTS ($V = 4, W = 4$)	64	9.56	9.3
ABC-PTS($FN = 4, MC = 64$)	256	7.45	7.2
ABC-PTS($FN = 4, MC = 256$)	1024	7.19	7
I-PTS	30	8.4	8.2
GD-PTS	1260	8	7.82
BFO-PTS	384	7.7	7.52
RS-PTS	1024	7.5	7.31
CR-New-PTS($V = 8, W = 4, V_a = 2$)	8	9.48	9.27
CR-New-PTS ($V = 16, W = 2, V_a = 4$)	16	9.21	9.04
CR-New-PTS ($V = 8, W = 4, V_a = 4$)	128	8	7.82
CR-New-PTS ($V = 16, W = 2, V_a = 8$)	256	7.17	7

With only 8 search processes in the CR-New-PTS technique, nearly the same PAPR reduction is achieved as with O-PTS using 64 search processes. However, when the number of search processes is 128 and 256, respectively, CR-New-PTS achieves the same PAPR reduction as GD-PTS with 1260 search processes and ABC-PTS with 1024 search processes. Overall, CR-New-PTS with 256 search processes provides a better PAPR value than all other methods.

4.3.2 BER Performance of the OFDM System

In order to evaluate the BER performance, an Additive White Gaussian Noise (AWGN) channel is used in all simulations, and the Signal-to-Noise Ratio (SNR) is expressed in terms of P_{avg}/N_0, N_0 being the power spectral density of the noise and P_{avg} the average power of the received signal. Figures 4.7 and 4.8 illustrate the BER curves obtained for the CR-New-PTS technique with 256 search processes and for O-PTS with 32,768 search processes, considering the effect of a power amplifier and using QPSK and 16-QAM modulations during the simulation. The IBO (Input Back-Off) value remains a critical factor in system

performance in terms of BER. Figure 4.8 shows that, when QPSK modulation is used, the BER performance of CR-New-PTS for IBO = 3 dB and IBO = 6 dB corresponds to SNR values of 17.5 dB and 21.5 dB, respectively, at $BER = 10^{-7}$. Similarly, the BER performance of O-PTS for IBO = 3 dB and IBO = 6 dB corresponds to SNR values of 17.3 dB and 21.3 dB, respectively, at $BER = 10^{-7}$. In this case, the CR-New-PTS exhibits nearly the same BER performance as O-PTS. Furthermore, Figures 4.7 and 4.8 show that the performance of QPSK modulation exceeds that of 16-QAM by approximately 4 dB.

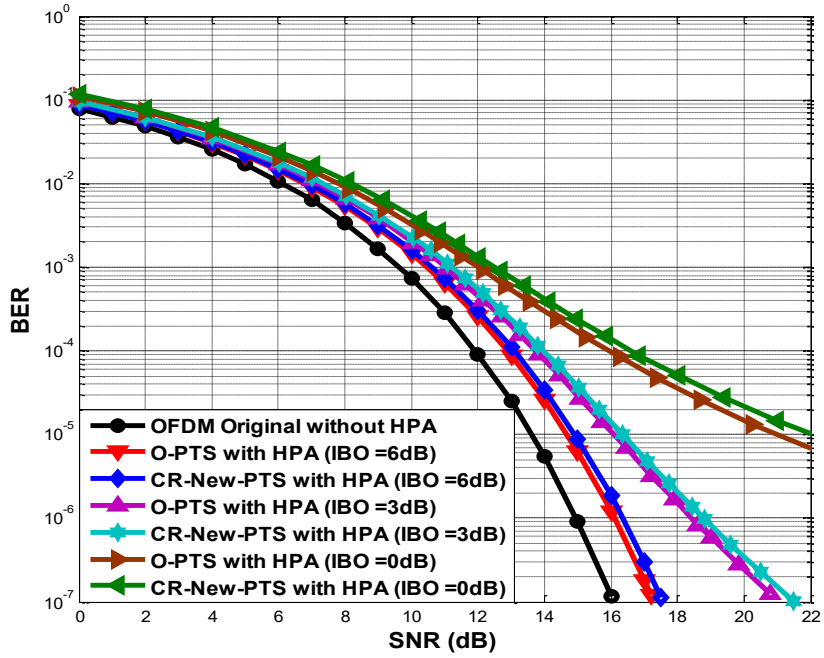

Figure 4.7: BER performance of the OFDM system using CR-New-PTS and O-PTS with QPSK modulation, when an HPA is applied over an AWGN channel.

In the Rayleigh multipath channel scenario, the BER curves are illustrated in Figures 4.9 and 4.10 using the same simulation parameters as in the AWGN channel case. A total of 16 channel paths are considered. Figure 4.9 reveals that, when QPSK modulation is used, the BER performance of CR-New-PTS for IBO = 3 dB and IBO = 6 dB corresponds to SNR values of 28.1 dB and 24.4 dB, respectively, at $BER = 10^{-7}$, the BER performance of O-PTS for IBO = 3 dB and IBO = 6 dB corresponds to SNR values of 27.4 dB and 24.1 dB, respectively.

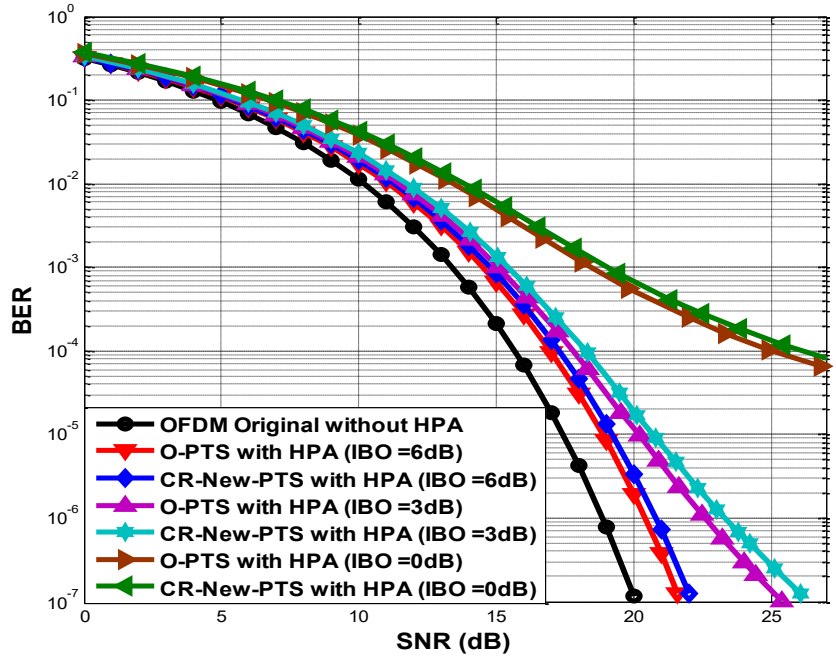

Figure 4.8: BER performance of the OFDM system using CR-New-PTS and O-PTS with 16-QAM modulation, when an HPA is applied over an AWGN channel.

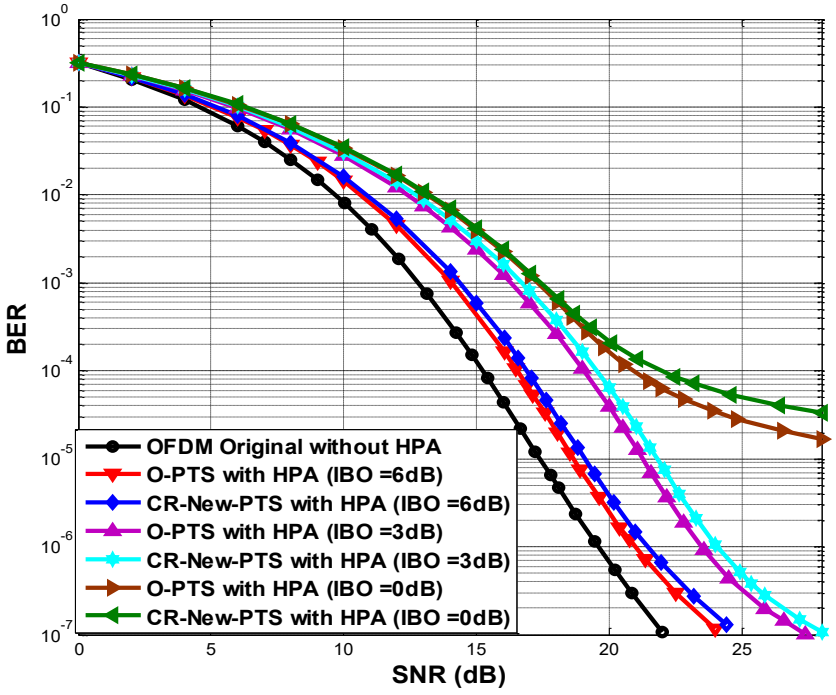

Figure 4.9: BER performance of the OFDM system using CR-New-PTS and O-PTS with QPSK modulation, when an HPA is applied over a Rayleigh channel.

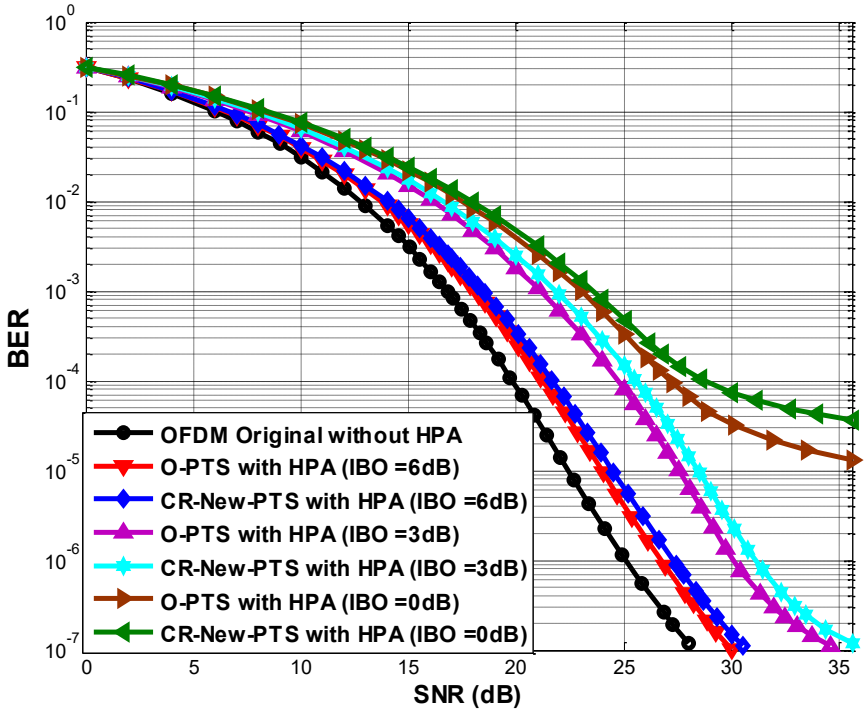

Figure 4.10: BER performance of the OFDM system using CR-New-PTS and O-PTS with 16-QAM modulation, when an HPA is applied over a Rayleigh channel.

Figure 4.10 shows that, when using 16-QAM modulation, the BER performance of CR-New-PTS for IBO = 3 dB and IBO = 6 dB corresponds to SNR values of 35.6 dB and 30.5 dB, respectively. Similarly, the BER performance of O-PTS for IBO = 3 dB and IBO = 6 dB is 34.6 dB and 30 dB, respectively, at $BER = 10^{-7}$. Moreover, IBO = 0 dB leads to a degradation in the performance of both CR-New-PTS and O-PTS for QPSK and 16-QAM modulations, in both the AWGN channel and the Rayleigh multipath scenario.

4.4 Conclusion

This topic addresses a fundamental issue in multicarrier communication systems (OFDM), namely the high Peak-to-Average Power Ratio (PAPR), which is one of the major challenges negatively impacting power amplifier efficiency and leading to signal distortion. To overcome this issue, the authors propose a novel technique called CR-New-PTS, aimed at reducing the computational complexity associated with conventional PAPR reduction methods while maintaining high system performance. Through simulation results, the proposed technique demonstrated its ability to achieve comparable if not superior performance compared to other approaches such as O-PTS and ABC-PTS, despite utilizing significantly fewer search processes. This contributes to a considerable reduction in execution time and computational

cost. The performance was evaluated under different channel conditions, including the AWGN channel and Rayleigh multipath fading, using QPSK and 16-QAM modulations. The results showed that QPSK outperforms 16-QAM in terms of Bit Error Rate (BER) by approximately 4 dB. Furthermore, the results revealed that the Input Back-Off (IBO) value plays a key role in system performance, as low IBO values (e.g. 0 dB) cause significant performance degradation. Therefore, the CR-New-PTS technique proves to be effective in achieving an optimal trade-off between PAPR reduction and computational complexity, making it a promising candidate for future wireless communication systems.

Conclusion general

At the end of this work, we have thoroughly addressed one of the most significant technical challenges facing the efficiency of Orthogonal Frequency Division Multiplexing (OFDM) systems, namely the high Peak-to-Average Power Ratio (PAPR) problem. This issue has a direct negative impact on the performance of power amplifiers in wireless communication systems, as it forces the amplifier to operate in the nonlinear region, which leads to signal distortion, spectral spreading, adjacent channel interference, and decreased power efficiency. Therefore, developing effective techniques to mitigate PAPR is essential, especially in the context of Fifth Generation (5G) networks that require high data rates, low latency, and reliable performance.

Among the existing approaches to PAPR reduction, this study focused on the Partial Transmit Sequence (PTS) technique, which is widely recognized for its ability to significantly reduce PAPR without degrading signal quality. However, the conventional PTS method suffers from high computational complexity due to the exhaustive search for optimal phase factors. To overcome this limitation, we proposed a low-complexity version of the PTS technique aimed at reducing the computational burden while maintaining satisfactory PAPR reduction performance. The proposed method was evaluated through various simulation scenarios using different system parameters. The obtained results demonstrated that our improved PTS approach effectively reduces PAPR with a noticeable decrease in computational complexity compared to traditional methods, making it a practical solution for real-time applications in 5G systems.

Furthermore, this research opens promising future perspectives, such as the potential integration of advanced metaheuristic optimization algorithms (like Genetic Algorithms or Particle Swarm Optimization) or the use of Artificial Intelligence techniques to further improve phase factor selection and minimize processing time while achieving even better performance.

In conclusion, we believe that this work represents a modest but meaningful contribution to enhancing the efficiency of modern wireless communication systems. We hope it will serve as a useful reference for future research aiming to develop more efficient and practical solutions to address the PAPR challenge in OFDM-based technologies.

Bibliographies

[1] Orthogonal Frequency Division Multiplexing, 3 488 445, US. patent, 1970.

[2] S. Weinstein and P. Ebert. Data transmission by frequency-division multiplexing using the discrete fourier transform. Communication Technology, IEEE Transactions on, 19(5) :628–634, October 1971.

[3] R. V. Nee and R. Prasad.OFDM for Wireless Multimedia Communications. Artech House,Inc., 2000.

[4] Digital Audio Broadcasting (DAB); DAB to Mobile, Portable and Fixed Receivers, February 1995.

[5] EN ETSI. 302 304 v1. 1.1 (2004-11) :"Digital Video Broadcasting (DVB) : Transmission System for Handheld Terminals (DVB-H)". European Telecommunication Standard, 2004

[6] EN ETSI. 302 755 v1. 2.1 (2010-10)"Digital Video Broadcasting (DVB). Frame Structure Channel Coding and Modulation for a Second Generation Digital Terrestrial Television Broadcasting System (DVB-T2), 2010.

[7] TS ETSI. 101 475 V1. 3.1 (2001-12), Broadband Radio Access Networks (BRAN) ; HIPERLAN type 2 ; physical (PHY) layer. 2001.

[8] TS ETSI. 101 388 V1. 3.1 (2002–05). Asymmetric Digital Subscriber Line (ADSL)-European specific requirements, 2002.

[9] Erik Dahlman, Stefan Parkvall, and Johan Skold. 4G : LTE/LTE-advanced for mobile broadband. Academic press, 2013.

[10] S.Merchan, A.G. Armada, and J.L.Garcia. "OFDM performance in amplifiernonlinearity", IEEE Transactions on Broadcasting, (1998), 44(1), pp.106-114.

[11] H.Merah, D.Slimani, and M.F.Alsharekh. "PAPR reduction in SFBC-MIMO-MC-CDMA

systems using method of attenuation complex chips", IEEE 3rd International Conference

on Control, Engineering and Information, Tlemcen, Algeria , May 2015, pp. 1-5.

[12] C. Siclet. Application de la th´eorie des bancs de filtres `a l'analyse et `a la conception de modulations multiporteuses orthogonales et biorthogonales. PhD thesis, Rennes 1 University, France, 2002.

[13] ALexandre SKRZYPCZAK. Contribution ´a l' ´etude des Modulations multiporteuses

OFDM/OQAM et OFDM Sur´echantillonn´ees. PhD thesis, Universit´e de Rennes 1, Novembre 2007.

[14] Haijian Zhang. Modulation multiporteuses `a base de bancs de filtres (FBMC) pour laRadio Cognitive. PhD thesis, Conservatoire National des Arts et Metiers, CNAM, Paris,Novembre 2010.

[15] D. Pommier, "Description and features of the cofdm systems," in Proc. IEE Colloquium on Terrestrial DAB - Where is it Going ?, pp. 4/1–4/6, 17 Feb 1993.

[16] M. Aldinger, "Multicarrier COFDM scheme in high bitrate radio local area networks," in Proc. th IEEE International Symposium on Personal, Indoor and Mobile Radio Communications Wireless Networks - Catching the Mobile Future, vol. 3,

pp. 969–973, 18–23 Sep 1994.

[17] S.Ma, et al. "Blind symbol synchronization based on cyclic prefix for OFDM systems",IEEE Transactions on Vehicular Technology, (2008), 58(4), pp. 1746-1751.

[18] K.Anoh, C.Tanriover, and B.Adebisi. "On the optimization of iterative clipping andfiltering for PAPR reduction in OFDM systems", IEEE Access, (2017), 5, pp. 12004-12013.

[19] D.H.Park, and H.K.Song. "A new PAPR reduction technique of OFDM system withnonlinear high power amplifier", IEEE Transactions on Consumer Electronics,(2007), 53(2), pp. 327-332.

[20] N.Escalera et al. "Ka-band, 30 watts solid state power amplifier", IEEE MTT-SInternational Microwave Symposium Digest (Cat. No. 00CH37017), Boston, USA, June2000, 1, pp. 561-563.

[21] S. Ragusa. "Ecrêtage Inversible pour l‟Amplification Non-Linéaire des Signaux OFDMdans les Terminaux Mobile", Thèse de Doctorat, université de Joseph FOURIER, Juin2006.

[22] N.T.Hieu, S.W.Kiom, and H.G.Ryu. "PAPR reduction of the low complexity phaseweighting method in OFDM communication system", IEEE Transactions on ConsumerElectronics, (2005), 51(3), pp. 776-782.

[23] S.HUSSAIN. "Peak to Average Power Ratio Analysis and Reduction of Cognitive Radio

Signals", Thèse de Doctorat, Institut d'Electronique et de Télécommunications de Rennes, Octobre 2009.

[24] M. L. Diallo. "Contribution aux techniques dites d'ajout de signal pour la Réduction duFacteur de Crête des signaux OFDM", Thèse de Doctorat, École doctorale Matisse, Juin2016.

[25] J. Tellado-Mourelo. "Peak to Average Power Reduction for Multicarrier Modulation",PhD thesis, Standford University, 1999.

[26] H.Abulkader. "Application de réseaux de neurones à des chaînes de transmissionnumérique par satellite gradient naturel", Thèse de Doctorat, Institut NationalPolytechnique de Toulouse, 2003.

[27] S. Bouchired. "Equalization of time-varying non-linear channels using neural networks:Application to the satellite mobile channel", Thèse de Doctorat, Institut nationalPolytechnique de Toulouse, 1999.

[28] A.A.Saleh. "Frequency-independent and frequency-dependent nonlinear models of TWTamplifiers", IEEE Transactions on communications, (1981), 29(11), pp. 1715-1720.

[29] C.Rapp. "Effects of HPA-nonlinearity on a 4-DPSK/OFDM-signal for a digital soundbroadcasting signal", Second European Conference on Satellite Communications, Liege,Belgium, October 1991, pp. 179-184.

[30] A.Chaker. "Influence de l‟amplificateur de puissance sur une chaîne de transmission multiporteuses: prise en compte de l‟effet mémoire", Thèse de Doctorat, Université CergyPontoise, Juillet 2004.

[31] D.Guel. "Étude de nouvelles techniques de réduction du «facteur de crête» àcompatibilité descendante pour les systèmes multiporteuse", Thèse de Doctorat, Universitéde Rennes1, Novembre 2009.

[32] A .Kellet. "Conception et réalisation d'un amplificateur RF à haut rendement énergétique", Thèse de Doctorat, École de technologie supérieure Montréal, Juin 2015.

[33] M.O'Droma, N.Mgebrishvili, and A.Goacher. "New percentage linearization measures ofthe degree of linearization of HPA nonlinearity", IEEE communications letters, (2004),8(4), pp. 214-216.

[34] F. Dowla. "Handbook of RF and Wireless Technologies", Book, Newnes, 1 edition,November 2003.

[35] M. K. Kazimierczuk. "RF Power Amplifiers", Book, Wiley, December 2008.

[36] H.Ku, and J.S.Kenney. "Behavioral modeling of nonlinear RF power amplifiers considering memory effects", IEEE transactions on microwave theory and techniques,(2003), 51(12), pp. 2495-2504.

[37] D. Su. "CMOS RF Power Amplifiers: Nonlinear, Linear, Linearized", tech. rep,Sunnyvale, California, November 2002

[38] S. H. Han and J. H. Lee, "An Overview of Peak-to-Average Power Ratio Reduction Techniques for Multicarrier Transmission," IEEE Wireless Communications, vol. 12, no. 2, pp. 56–65, Apr. 2005.

[39] T. Jiang and Y. Wu, "An Overview: Peak-to-Average Power Ratio Reduction Techniques for OFDM Signals," IEEE Trans. on Broadcasting, vol. 54, no. 2, pp. 257–268, Jun. 2008.

[40] Y. Rahmatallah and S. Mohan, "Peak-To-Average Power Ratio Reduction in OFDM Systems: A Survey and Taxonomy," IEEE Commun. Surveys & Tutorials, vol. 15, no. 4, pp. 1567–1592, 2013.

[41] L. Wang and C. Tellambura, "A Simplified Clipping and Filtering Technique for PAPR Reduction in OFDM Systems," IEEE Signal Process. Lett., vol. 12, no. 6, pp. 453–456, Jun. 2005.

[42] S. H. Müller and J. B. Huber, “OFDM with reduced peak-to-average power ratio by optimum combination of partial transmit sequences,” Electronics Letters, vol. 33, no. 5, pp. 368–369, 1997.

[43] L. Wang and C. Tellambura, “Analysis of clipping noise and tone reservation algorithms for peak reduction in OFDM systems,” IEEE Transactions on Vehicular Technology, vol. 57, no. 3, pp. 1675–1694, 2008.

[44] P.Varahram, W.F. Al-Azzo, and B.M.Ali. "A low complexity partial transmit sequence scheme by use of dummy signals for PAPR reduction in OFDM systems", IEEE Transactions on Consumer Electronics, (2010), 56(4), pp. 2416-2420.

[45] L.J.Cimini, N.R.Sollenberger. "Peak-to-average power ratio reduction of an OFDM signal using partial transmit sequences ", IEEE Communication Letters, (2000), 4 (3), pp. 86–88.

[46] S.H.Han, J.Lee. "PAPR reduction of OFDM signals using a reduced complexity PTS technique", IEEE Signal Processing Letters, (2004), 11(11), pp. 887–890.

[47] X.Cheng, D.Liu, S.Feng, et al. "PTS based on discrete artificial bee colony algorithm for PAPR reduction in OFDM systems", Electronics Letters, (2018), 54(6), pp. 397–398.

[48] R.Manjith, M.Suganthi. "A sub-optimal PTS algorithm based on bacterial foraging optimization technique for PAPR reduction in MIMO-OFDM system", Journal of Theoretical and Applied Information Technology, (2013), 57 (2), pp. 261–268

[49] N.Shi, S.Wei. "A partial transmit sequences based approach for the reduction of peak-to-average power ratio in FBMC system", IEEE 25th Wireless and Optical Communication Conference (WOCC), Chengdu, China, May 2016, pp. 1-3.

[50] S.H. Deng et al. "Modified PTS-based PAPR Reduction for FBMC-OQAM Systems", in Journal of Physics: Conference Series, (2017), 910, p. 012057.

[50] H.L. Kaiming et al. "PAPR reduction for FBMC-OQAM systems using P-PTS scheme", The Journal of China Universities of Posts and Telecommunications, (2015), 22(6), pp. 78–85.

[51] H.Merah, M.Mesri, and L.Talbi. "Complexity reduction of PTS technique to reduce PAPR of OFDM signal used in a wireless communication system", IET Communications, (2019), 13(7), pp. 939-946.

[52] A.Goel, P.Gupta and M.Agrawal. "Concentric circle mapping based PTS for PAPR reduction in OFDM without side information", IEEE 6th International conference on Wireless Communication and Sensor Networks, Allahabad, India, December 2010, pp. 1-4.

[53] H.Kim et al. "A pilot symbol pattern enabling data recovery without side information in PTS-based OFDM systems", IEEE Transactions on Broadcasting, (2011), 57(2), pp. 307-312.

[54] L.Yang et al. "PAPR reduction using low complexity PTS to construct of OFDM signals without side information", IEEE Transactions on Broadcasting, (2011), 57(2), pp. 284-290.